# Interactive comment on "Spatial distribution of water level impact to back-barrier bays" by Alfredo L. Aretxabaleta et al.

**Anonymous Referee #1**

**Response to Reviewers, comments in plain text, response in bold**

5 The authors have proposed a novel approach to combine observed data and numerical model results for spatial characterization of water level transfer inside Barnegat Bay. They use dimensional characteristics of the bay to ensure this combination occurs in a physically consistent way. The idea is interesting and the manuscript is generally well-written, so I think it deserves publishing in NHESS after a major revision. Details are provided below:

*Major:*

10 - In page 5, with a harmonic assumption for water level and velocity, jumps into a giant equation (I wish there was an equation number I could refer to!). There is no way I can evaluate the robustness of approach, without knowing the exact steps and detailed assumption made here. I suggest, either providing enough details to enable proving the accuracy of equations, or if there is not enough room in the main manuscript (which I think is the case) add supplementary materials and provide the detailed steps in that document.

15 **The development of the equations is now provided in an appendix (Appendix A). Originally, we decided to exclude them as they take up a lot of space. Also, the equation numbers have been added to the text.**

- M2 is taken as a proxy for internal frictional effects (Page 7, Line 2). As far as I understand, overtides (i.e. M4) are better proxies for internal frictional effects. It's already been mentioned in the manuscript (Page 7, line 17) that remaining frequency bands exhibit smaller fluctuations, but their variability given forcing still contains useful information. Please,

20 revise or justify this approach.

**The $M_4$ tidal constituent is generated as a non-linear response to $M_2$ tidal forcing. The magnitude of the $M_4$ is partially a result of the energy loss from $M_2$ through friction but also associated with other nonlinearities. In general, the $M_4$ is a result of asymmetries in the duration of ebb and flood. There is no external solar or lunar forcing at the $M_4$ frequency. Thus, as the Reviewer mentions, the $M_4$ and other overtides might be related to internal frictional**

25 **effects in terms of where the $M_4$ is generated. In fact, the tidal constituent more associated with frictional generation is $M_6$ rather than $M_4$. The issue is that the $M_4$ also propagates as a normal tidal wave and the magnitude at a specific location can be the result of either local generation or propagation and it will also be subject to attenuation by friction. The spatial changes in the $M_2$ tidal constituent inside the bays are a direct consequence of the frictional dissipation of tidal energy through friction (Redfield, 1980). Therefore, the changes in $M_2$ amplitude are a better**

30 **metric for the frictional effects inside the bay.**

*Minor:*

- In Page 1, Line 33: there are many more recent citations to be cited here, including the revised version of this report in 2013. Also, see the followings for example:

* Rahmstorf (2017) Rising hazard of storm-surge flooding, PNAS, https://doi.org/10.1073/pnas.1715895114

5    * Wahl et al. (2017) Understanding extreme sea levels for broad-scale coastal impact and adaptation analysis, Nature Communications volume 8, Article number: 16075.

**We have added the references mentioned by the Reviewer.**

**Ln 30-32: "Both hurricanes and winter storms affect coastal populations, infrastructure, and natural resources along the coastal bays of the United States (Nicholls et al., 2007, 2014; Rahmstorf, 2017; Wahl et al., 2017)."**

10    - In Page 2, Line 32: The following paper may be cited to define the term nuisance flooding for interested readers. * Moftakhari et al. (2018) What is nuisance flooding? Defining and monitoring an emerging challenge, Water Resources Research 54 (7), 4218-4227.

**The reference has been added to the text.**

**Ln 63-65: "The method will be useful for coastal hazard assessment assisting in the management of nuisance flooding**

15    **(Moftakhari et al., 2018) and providing spatial differences in vulnerability to perigean spring tides (king tides) and planning for flooding in response to storms of different durations."**

- In Page 3, lines 3-4: cite more recent literature, as you are pointing to the gap and we need to make sure the gap has not been filled since 2000.

**We have added recent references to the text to show the continuing coastal focus. For instance:**

20    - **Neumann, B., Vafeidis, A.T., Zimmermann, J. and Nicholls, R.J.: Future coastal population growth and exposure to sea-level rise and coastal flooding-a global assessment. PloS one, 10(3), p.e0118571, 2015.**
   - **Vitousek, S., Barnard, P.L., Fletcher, C.H., Frazer, N., Erikson, L. and Storlazzi, C.D.: Doubling of coastal flooding frequency within decades due to sea-level rise. Scientific reports, 7(1), p.1399, 2017.**

   **Ln 34-38: "While flooding in the mainland side of back-barrier bays has severe socio-economic implications, most of**

25    **the coastal hazard evaluations (Gornitz et al., 1994; Thieler and Hammar-Klose, 1999; Klein and Nicholls, 1999; Kunreuther et al., 2000; Neumann et al., 2015; Vitousek et al., 2017) have focused in open-coast areas. Vulnerability evaluation of coastal areas around back-barrier bays requires extensive knowledge of the main hazard sources and their physical controls."**

- Please use different notation in harmonic assumption for amplitude and actual fluctuating variable (i.e. saying

30    u=u*exp(iwt) is confusing)

**We have improved the notation accordingly and differentiated between the amplitude and the fluctuating variable. For instance, Ln 120-121: "Assuming $\eta = \tilde{\eta}e^{i\omega t}$ and $u = \tilde{u}e^{i\omega t}$, where $\tilde{\eta}$ and $\tilde{u}$, represent the magnitude of the water level and velocity oscillations, respectively."**

- In Page 5, Line 3: please be specific what kind relationship would be described by phi parameter (linear? nonlinear?...)

The relationship that the parameter phi represents is a linear relationship that is consistent with the linear equation described in the text. We have clarified this characteristic in the text.

Ln 117-119: "$\phi_{LEI}$, $\phi_{BI}$, $\phi_{breach}$, $\phi_{PPC}$ are the linear frequency-dependent relationships between the water levels at offshore proxy stations (Sandy Hook or Atlantic City) and the water level just offshore of Little Egg Inlet, Barnegat Inlet, the breach at Mantoloking caused by Sandy, and Point Pleasant Canal."

Reference:

Redfield, A.C., 1980. "The tides of the waters of New England and New York", 109 pp., doi:10.1575/1912/1136, https://hdl.handle.net/1912/1136

3

# Interactive comment on "Spatial distribution of water level impact to back-barrier bays" by Alfredo L. Aretxabaleta et al.

Anonymous Referee #2

## Response to Reviewers, comments in plain text, response in bold

_GENERAL COMMENTS_

The paper is impressive and can be influential, with some excellent ideas and its broad perspective based on observations, detailed numerical modeling, analytical modeling, and also possible extension nationwide using an ADCIRC tide constituent database. However, the analytical developments are dense and could be explained better for a less technical reader. Also, and most importantly, the discussion of potential use with ADCIRC tide modeling results datasets in storm hazard assessment needs work. I believe a major shortcoming there is the neglect of local wind setup in storms. Back-bays can have a wide range of inlet sizes, bay area, and often have shallow water depths, and as a result, can have an important role for local wind setup in storms. The paper can acknowledge this, if the authors agree, and it will be a stronger paper. As a result, I recommend major revision.

**The reviewer is completely correct. There was an error in the calculations of the local wind setup. The formulas were fine but there was an error on the implementation of the formulas. After the error was corrected, the effect of the wind was substantially bigger (5-10 times). The new results have been included and the paper makes a much better argument about the importance of wind setup thanks to the suggestions made by the reviewer.**

**We included the wind effects on the bay in two sections of the paper. Section 4.2 and 4.3 include the methodology, while Section 5.2 includes the results of the wind effect on the bay. We have added the wind effects in the discussion of the ADCIRC results as the Reviewer suggested.**

**Ln 243-251: "The resulting effect of the wind setup (or set-down) was small (less than 0.1 m with an along-bay wind stress of 0.1 Pa) for most of the domain (Figure 8). The estimate assumed a linear friction of the same magnitude as in Section 5.1 ($r=0.021$ m/s). Under persistent wind stress of 0.1 Pa (about 8 m/s wind speed) in the along-bay direction, the resulting setups varied depending on the frequency considered. Setup magnitudes over 0.2 m were estimated for the 5-day period wind (Figure 8c), while under half of that magnitude was achieved for the 2-day persistent wind (Figure 8b), and much smaller water level setup (peak smaller than 0.1 m) was estimated for the sea breeze (Figure 8a). During extreme events like Hurricane Sandy, under intense wind stress, two additional effects should be considered: the depth of the bay increases by the transfer of offshore surge resulting in altered setup response (Section 4.2), and the frictional effect is enhanced (a larger linear friction would be needed) by the presence of wave-induced roughness."**

**Ln 273-282: "The wind setup effect inside the bay due to local wind can also be estimated for Hurricane Sandy using the approach in Section 4.2. Maximum wind stress during the storm was about 1 Pa. To obtain a maximum effect (worst-case scenario) the wind was assumed to be persistently in the along-bay direction and that maximum stress was maintained for the duration of the storm. The maximum resulting water level considering the Wong and Moses-Hall method is linear with regard to wind stress magnitude (Figure 7b) and would have been 10 times larger than the setup in Figure 8b. The maximum wind setup would have been between 1 and 2 m, which was of the same order of magnitude as the surge produced from offshore sources. The cross-bay contribution to the wind setup during Sandy was comparatively small as wind direction was predominantly along-bay. Surge estimates from simple analytical formulations (State Committee for the Zuiderzee, 1926; Pugh, 1987) that do not consider storm duration produce similar magnitude results and are also dependent on the frictional response of the bay."**

**Ln 314-319: "The effect of local wind setup will also need to be added to the ADCIRC-based estimate, especially during severe storms. The approach discussed in Section 5.2 or even a simpler surge calculation (e.g., from the steady state vertically averaged momentum equations, as in Pugh (1987), from the traditional report of the State Committee for the Zuiderzee (1926), or the updated frequency domain equivalent from Reef et al., 2018) could be used and the resulting**

elevation could be added to the offshore transfer estimate obtain based on the ADCIRC tides. Thus, the production of bay water level predictions will require accurate wind forecast products."

*SPECIFIC COMMENTS*
ABSTRACT
A minor comment – text refers to "Inlet geometry and bathymetry" as being important in semi-enclosed bays - isn't bay area also important?
**Bay geometry was included two sentences before. We have added bay area to that sentence so that it reads: "Bay area and inlet geometry and bathymetry primarily regulate the magnitude of the transfer between open ocean and bay."**
The abstract says storm transfers were from 70-100% but I see ~50% in some cases- eg MAN at 5-day period, WAR at 2-days. So this should be revised to 50-100%.
**Agreed. It has been revised according to the Reviewer's suggestion.**
**Ln 16-18: "Model water level transfers match observed values at locations inside the Bay in the storm frequency band (transfers ranging from 50-100%) and tidal frequencies (10-55%)."**
The last several sentences of the abstract don't seem very consistent with the paper's discussion- differing topics are discussed. Also where is mention of the ADCIRC based transfer estimates?
**The second to last sentence has been removed and an alternative has been added that explains the ADCIRC-based approach potential for expansion to other areas. It reads:**
**Ln 21-22: "An extension of the methodology that takes advantage of the ADCIRC tidal database for the east coast of the United States allows for the expansion of the approach to other bay systems."**
INTRO vs METHODS
A part of the intro's literature review says that wind controls backbay currents (Garvine 1985). But in the methods, the approach uses tidal current M2 are a proxy for bed friction.
**While wind has a large influence in back-bay current variability, the character of the wind response is less predictable. The total current is mainly a result of the combined effect of wind and tides. In the absence of wind, the tides will always be there. Estimating bottom friction based only on the M2 tidal current might underestimate friction in cases of large wind currents. In reality, the linear friction estimate is based on the match of the M2 tidal amplitude in the numerical model and the observations and as such it includes any components of the velocity that has affected the observations and resulted in the measured water level signals. This point has been clarified in the text by adding:**
**Ln 165-170: "As most of the water level variability in the bay is associated with the M2 semidiurnal tidal constituent (Figure 3) and the distribution of the tide has been properly validated in the numerical simulations (Defne and Ganju, 2015), we can take the spatial distribution of the M2 tidal amplitude as a proxy for the internal frictional effects in the bay. Bottom friction caused by both wind driven and tidal effects is considered in the numerical simulations. By adjusting the water level based on the numerical M2 spatial distribution, we are approximating the complete frictional characteristics of the bay."**
Section 4.2, p. 6 – on wind's influence – analytical model – instead of saying "angular frequency" would it be more clear to say "cyclic frequency"? The figures show "cycles/day" and "angular frequency" just is a little confusing to me. It isn't measured as an angle (degrees), it's measured by cycles.
**We have included the suggestion to avoid confusion. It now reads, Ln 145: "… ω is the cyclic (angular) frequency".**

Here, you also might refer to the two different stresses as "dynamic stress" (tau_s I believe) and "kinematic stress" (tau_w), as well as in the figure caption. It would have helped me a little in understanding the figure's values (values of order 1000) as I typically think in terms of dynamic stress in Pascals.
**We have changed the text accordingly.**
**Ln 142-144: "$\tau_s$ and $\tau_b$ are the surface and bottom dynamic stresses, respectively; and $\rho_0$ is the water density. $\tau_w = {}^{\tau_s}\!/\rho_0$ is the spatially invariant kinematic wind stress and $r$ is a linearized bottom friction."**
**Ln 148-149: "$\widetilde{\tau_w}(\omega)$ represents the magnitude of the kinematic wind stress that results in water level fluctuations at a specific frequency."**

I am a bit confused about why tau is written as a function of omega (parenthetically) here so it is probably a good thing to explain things more. I see wind stress and frequency as being independent variables.

**The wind stress represented here is the magnitude of the wind oscillations that result in water level fluctuations at a specific frequency.**

Also, does the denominator really include cos(Lx) here? I see L as being on the order of 10000m and x being from 0 to 10000 (meters).

**That is a typo. The equation should read cos(kL) instead. It has been corrected in the text.**

Section 6.1- aspects regarding sandy don't seem very useful here – see points below on local wind setup

"this far" – requires a minor revision to "thus far" I believe Section 6.2 **It has been corrected**

A very interesting idea and impressive analysis and results Section 6.3 **Thanks. We believe it has the potential to help in the prediction of bay water level hazards.**

Seems to be a fairly ingenious approach! are all US backbays really available and well-resolved in the ADCIRC tide data? In this case there is a large inlet that controls results, but I expect there are tougher cases.

**Clearly not all back-barrier bays are well resolved in the tidal database, as some are relatively small. The ADCIRC model run provides resolutions down to around 50m in the latest database. The ADCIRC group keeps improving the resolution of their products. It is likely that their solutions will soon improve their quality and resolution, thus having the potential for providing even better back-bay response. The process of evaluating the quality of the current approach is underway, but so far it exhibits great potential.**

A little more elaboration or demonstration here might be useful – it's the final landing point of the paper and seems like it could be helpful to illustrate this potential application with more detail.

**The paper introduces the methodology based on the ADCIRC tides for the creation of offshore transfer estimates. The potential use for water level prediction in bays requires very careful calibration and skill assessment. The transfer maps represent an approximation to the average bay response to offshore forcing and specific events can depart significantly from the average response. Effects like overtopping of the barrier island, wave setup and runup, intense local wind setup, changes in frictional characteristics during a storm cannot be adequately predicted with the approach and need to be carefully included in the application to water level forecast.**

The claim in the paper seems to be that local wind setup is small and negligible for storms, relative to transfer of offshore surge. The maximum wind setup mentioned is only 20cm (p10, line16). This all seems surprising to me, as I have learned that (large, shallow) backbay surge is often strongly influenced by local winds.

**The reviewer is completely correct. There was an error in the calculations of the local wind setup. The formulas were fine (except from the typo mentioned above). The error was on the implementation of the formulas. After the error was corrected, the effect of the wind was much bigger (5-10 times). The maximum wind setup is now between 1 and 2 m. The text was changed accordingly. The new Figure 8 shows the same pattern, but the magnitude is much bigger:**
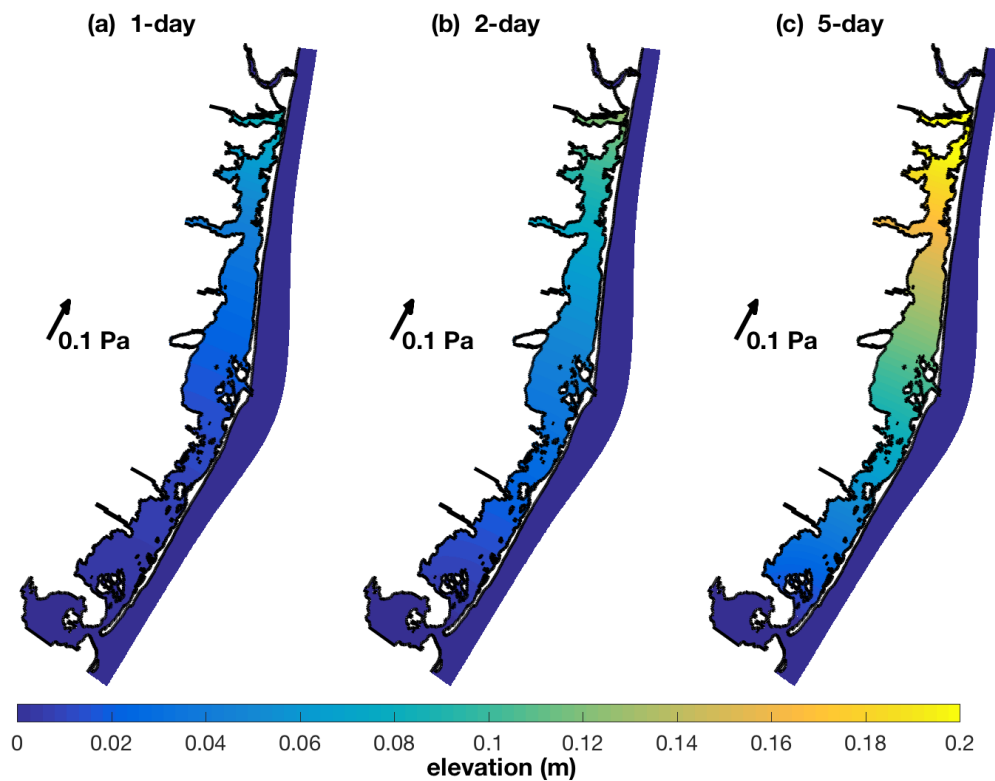
**New Figure 8:** Local wind setup inside the bay based on the Wong and Moses-Hall (1998) formulation for a wind stress of 0.1 Pa at specific periods: (a) wind with a 1-day period (e.g., sea breeze); (b) 2-day wind; and (c) 5-day wind.

The text has been modified to read:
**Ln 245-248: "Under persistent wind stress of 0.1 Pa (about 8 m/s wind speed) in the along-bay direction, the resulting setups varied depending on the frequency considered. Setup magnitudes over 0.2 m were estimated for the 5-day period wind (Figure 8c), while under half of that magnitude was achieved for the 2-day persistent wind (Figure 8b), and much smaller water level setup (peak smaller than 0.1 m) was estimated for the sea breeze (Figure 8a)."**

A challenge: the wind setup for the north winds prior to Sandy's landfall was studied, when winds blew water toward (fortunately!) the main inlet. How about computing and comparing setup for when the wind turned around and blew from the south after landfall, toward the nearly dead-end northern end of the bay? If we are interested in hazards, then this was the primary backbay damage-causing period of the event. I believe the local wind setup became quite large and abrupt at that time.

**The estimation of the wind setup during Sandy goes beyond the scope of the paper. The method can provide an estimate, but it is only a relative approximation. The available numerical model simulations of the area during Hurricane Sandy (Defne, Z., and Ganju, N.K., 2019, Collection of USGS Barnegat Bay hydrodynamic model simulations for Hurricane Sandy: U.S. Geological Survey data release, https://doi.org/10.5066/P99K85SW, available from the USGS Hurricane Sandy model portal: https://cmgdata.usgsportals.net/) represents a better estimate of the water level dynamics during the storm.**
**Nevertheless, we performed the estimation using the corrected implementation of the Wong & Moses-Hall formulation for both winds from the south (as requested) and also from the north. As the setup in the formulation is directly proportional to the wind stress, a wind stress of 1 Pa from the south would have resulted in elevations of around 2 m with the same pattern as in the new Figure 8 above. The formulation estimate for a wind stress of the same intensity (1 Pa) from the north is shown in the figure below. The figure shows the wind surge magnitude and provides an approximation for the gradient in water level caused by the wind stress. The total elevation would be the result of the addition of local wind setup plus offshore influence. So the elevation**

would match the offshore signal in the south near Little Egg Inlet and it would be a set-down (negative elevation with respect to MSL if no offshore elevation considered) in the north of the bay. Numerical model simulations (Defne and Ganju, 2019) show a similar pattern prior to Sandy's landfall. The magnitude of the wind effect (set-down with wind from the north, setup with winds from the south) is of the order of 1-2 m.
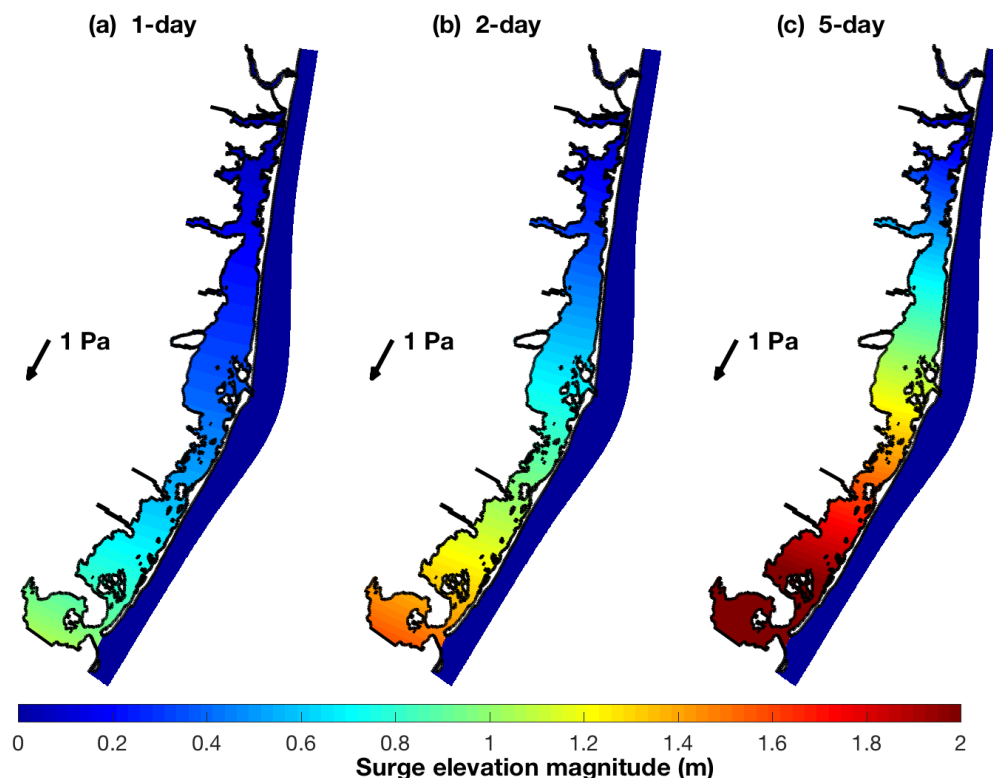


The focus of the present work is not the study of the water level dynamics during Hurricane Sandy, but rather the characterization of the average response of the bay to hazards. The Sandy example in the paper is mostly used as a discussion point.

During Sandy, water levels at Mantoloking rose about 2.5m in 12 hours when the wind rotated to come from the east and then south, reaching a maximum that was very close to the open ocean or Little Egg values (perhaps 30cm lower) (USGS station 01408168).
The analysis of observations and model results during Hurricane Sandy goes beyond the scope of the current study. The analysis of numerical model results for Barnegat Bay during Hurricane Sandy is underway and the basic characteristics are available at the USGS model portal (https://cmgdata.usgsportals.net/).

Does the analytical approach capture the effect of this large wind setup? If not, does this issue show that local wind setup can be a challenge for using the ADCIRC tide data to estimate storm hazards? Or, is Sandy too unusual of a case, in which case a nor'easter might be a better discussion point for the paper?
The new corrected results of the wind setup effects show that the approach described in the paper represents a match with the expected behavior. The addition of the ADCIRC-derived offshore transfer and the analytical wind setup has the potential for adequately estimating water level in back-barrier bays.

Using a back-of-the-envelope computation with an admittedly simpler, but well- established method to compute the wind setup for a 20m/s wind, 50km fetch, 2m deep backbay, if fully developed, is 2m (the Zuider-Zee equation, or similarly, making the computation using a steady state vertically averaged momentum budget - Pugh and Woodworth, 2014, p. 156 in Section 7.3 on Storm Surges). It takes only a matter of hours to fully develop. I agree on the 1Pa wind stress for Sandy- this is reasonable.

U=20m/s eg post-landfall Sandy
depth d=2m
fetch F=50000m
setup $S= 0.000002 * F * U^2 /g /d = 0.000002 * 50000* 400/9.8/2$ (Zuider-Zee equation) $S = 2m$ setup
I believe "L" in the analytical wind formulation is the basin length (for each of several small basins). I am computing the wind setup for a 50km long backbay, so perhaps using a longer fetch. But I believe this is appropriate as they are really not disconnected and the ~40km of the northern half of the model domain is strongly connected (not divided up into separate bays).

**The new corrected estimates are consistent with the values described by the reviewer. The modified text in Section 6.1 of the paper now reads:**

**Ln 273-282: "The wind setup effect inside the bay due to local wind can also be estimated for Hurricane Sandy using the approach in Section 4.2. Maximum wind stress during the storm was about 1 Pa. To obtain a maximum effect (worst-case scenario) the wind was assumed to be persistently in the along-bay direction and that maximum stress was maintained for the duration of the storm. The maximum resulting water level considering the Wong and Moses-Hall method is linear with regard to wind stress magnitude (Figure 7b) and would have been 10 times larger than the setup in Figure 8b. The maximum wind setup would have been between 1 and 2 m, which was of the same order of magnitude as the surge produced from offshore sources. The cross-bay contribution to the wind setup during Sandy was comparatively small as wind direction was predominantly along-bay. Surge estimates from simple analytical formulations (State Committee for the Zuiderzee, 1926; Pugh, 1987) that do not consider storm duration produce similar magnitude results and are also dependent on the frictional response of the bay."**

Sandy's surge might be viewed as having a "slow" 1-m surge with timescale of 3 days, plus a fast 1-m surge with a timescale of 1 day. I think for either case the ADCIRC- based transfer results in this paper suggest reduced transfer (maybe 60%; figure 10) for Mantoloking. In contrast, Sandy, the worst extreme event, shows that local wind effects lead to a similar surge there as seen offshore (perhaps 90% transfer). The transfer uncertainty estimates in Figure 11 (eg 4% in the 2-day storm band?) aren't evaluating this wind setup contribution, so aren't worth much.

**The reviewer is correct about the relative magnitude of the two effects. The text of the paper now includes a section describing the need to add the wind effect to the ADCIRC derived offshore transfer:**

**Ln 314-319: "The effect of local wind setup will also need to be added to the ADCIRC-based estimate, especially during severe storms. The approach discussed in Section 5.2 or even a simpler surge calculation (e.g., from the steady state vertically averaged momentum equations, as in Pugh (1987), from the traditional report of the State Committee for the Zuiderzee (1926), or the updated frequency domain equivalent from Reef et al., 2018) could be used and the resulting elevation could be added to the offshore transfer estimate obtain based on the ADCIRC tides. Thus, the production of bay water level predictions will require accurate wind forecast products."**

I think this local wind effect pushing water into the northern end of the bay is what causes the unexplained high transfer at Mantoloking (Figures 4-5) in the 2-day storm band. The model captures it because it includes wind forcing (and Sandy), but a tide- only model will not.

**Local wind setup is likely the reason for the enhanced transfer response during 2012. The magnitude of the storm is not as important as the fact that during 2012 the general pattern of the pressure systems over the Atlantic was conducive to wind in the along-bay direction. The effect was a potential enhancement of the local wind setup that showed up in Mantoloking and not in other stations (e.g., Waretown) because the water was able to setup in the northern part of the bay. The text in Section 5.1 now includes a sentence describing this:**

**Ln 205-209: "The model reproduced the enhanced transfer in the storm band at Mantoloking during 2012, suggesting a physical mechanism for the change that the model was able to capture but remains unexplained. The likely explanation is that the location of the Azores-Bermuda high-pressure system over the Atlantic in 2012 (Mattingly et al., 2012), associated with the negative phase of the North Atlantic Oscillation, resulted in average winds that lined up with the axis of the Bay and caused enhanced wind setup in the northern part of the bay."**

To conclude, I think the method presented would, for storms, often be low-biased for peak water level risk estimates, due to local wind setup. I suggest proceeding very carefully and validating storm hazard estimates, using observational data.... or evaluating case studies carefully to determine whether local

wind setup corrections or larger uncertainties can be added for the storm driven flood hazards. Underestimating storm-driven flood risk is worse than not estimating it at all.

REFERENCE Pugh and Woodworth, 2014, Sea Level Science, Second Edition, Cambridge University Press, Cambridge, UK.

**We greatly appreciate the reviewer's comments that forced us to review the implementation of the wind setup approach discovering an error. When the error was corrected, the method of combining the transfer of offshore fluctuations, via the analytical or ADCIRC-based approaches, and the local wind setup effect showed the potential for estimating bay water levels in response to tidal and storm forcing. We agree that under or over-estimation of storm driven flood risk has severe consequences for coastal hazard mitigation. Proper skill assessment of the methodology will be needed before the implementation of this kind of approach for storm impact. The text now includes a discussion of this point:**
**Ln 330-334: "Careful consideration needs to be given to the estimation of coastal hazards especially for the forecast of intense storm effects. The inclusion of meticulously validated methodologies that consider both offshore influences (e.g., using the transfer estimated from ADCIRC tides) and local wind setup (e.g., Wong and Moses-Hall, 1998; Reef et al., 2018) is necessary. Skill assessment of storm hazard estimates using adequate observations is critical to avoid producing under- or over-predictions of flooding and inundation."**

# Spatial distribution of water level impact to back-barrier bays

Alfredo L. Aretxabaleta[1], Neil K. Ganju[1], Zafer Defne[1], and Richard P. Signell[1]

[1] U.S. Geological Survey, Woods Hole, Massachusetts, 02543, USA

5 *Correspondence to*: Alfredo L. Aretxabaleta (aaretxabaleta@usgs.gov)

**Abstract.** Water level in semi-enclosed bays, landward of barrier islands, is mainly driven by offshore sea level fluctuations that are modulated by bay geometry and bathymetry, causing spatial variability in the ensuing response (transfer). Local wind setup can have a complementary role that depends on wind speed, fetch, and relative orientation of the wind direction and the bay. Bay area and inlet geometry and bathymetry primarily regulate the magnitude of the transfer between open ocean and bay. Tides and short-period offshore oscillations are more damped in the bays than longer-lasting offshore fluctuations, such as storm surge and sea level rise. We compare observed and modeled water levels at stations in a mid-Atlantic bay (Barnegat Bay) with offshore water level proxies. Observed water levels in Barnegat Bay are compared and combined with model results from the Coupled Ocean-Atmosphere-Wave-Sediment Transport (COAWST) modeling system to evaluate the spatial structure of the water level transfer. Analytical models based on the dimensional characteristics of the bay are used to combine the observed data and the numerical model results in a physically consistent approach. Model water level transfers match observed values at locations inside the Bay in the storm frequency band (transfers ranging from 550-100%) and tidal frequencies (10-55%). The contribution of frequency-dependent local setup caused by wind acting along the bay is also considered. The wind setup effect can be comparable in magnitude to the offshore transfer forcing during intense storms. The approach provides transfer estimates for locations inside the Bay where observations were not available resulting in a complete spatial characterization. An extension of the methodology that takes advantage of the ADCIRC tidal database for the east coast of the United States allows for the expansion of the approach to other bay systems. Detailed spatial estimates of water level transfer can inform decisions on inlet management and contribute to the assessment of current and future flooding hazard in back-barrier bays and along mainland shorelines.

## 1 Introduction

Back-barrier bays or coastal lagoons are common features along the coast of the United States. Their depths are usually on the order of a few meters and their horizontal extents are on the order of several tens of kilometers. They are often surrounded by highly populated areas and susceptible to intense human and environmental stressors. During storms, surge and larger than normal waves combine to inundate low-elevation areas, resulting in hazards to coastal communities. Both hurricanes and winter storms affect coastal populations, infrastructure, and natural resources along the coastal bays of the United States (Nicholls et al., 2007, 2014; Rahmstorf, 2017; Wahl et al., 2017).

1

Hazard assessments consist of a characterization of the spatial and temporal extent of damaging physical events and the determination of the specific characteristics of those events (Ludwig et al., 2018). While flooding in the mainland side of back-barrier bays has severe socio-economic implications, most of the coastal hazard evaluations (Gornitz et al., 1994;

45   Thieler and Hammar-Klose, 1999; Klein and Nicholls, 1999; Kunreuther et al., 2000; Neumann et al., 2015; Vitousek et al., 2017) have focused in open-coast areas. Vulnerability evaluation of coastal areas around back-barrier bays requires extensive knowledge of the main hazard sources and their physical controls.

Water level in the bays is mainly driven by offshore sea level fluctuations with additional effects by local wind and wave setups. The bay exchange with the ocean usually occurs through narrow inlets. The size of the inlet determines the frictional

50   effects and the amount of dampening offshore fluctuations encounter (Keulegan, 1967). Tides and short-period offshore oscillations tend to be more dampened in the bays than longer-lasting offshore fluctuations, such as storm surge and sea level rise.

Bay water level fluctuations are linked to offshore forcing especially at low frequencies, while wind acting directly over the bay is more connected to current fluctuations in the bay (Garvine, 1985). Chuang and Swenson (1981) determined that water

55   level changes at subtidal frequencies in Lake Pontchartrain were controlled by coupled coastal ocean-bay fluctuations. Wong and Wilson (1984) studied subtidal sea level fluctuations in Great South Bay and again found them primarily driven by bay-shelf coupling. In Delaware Bay, a bay-inlet system with a relatively large opening, Wong and DiLorenzo (1988) showed that remote effects dominate over local effects and that fluctuations at both tidal and subtidal frequencies in connected bays of the Delaware Bay system were forced by shelf sea level.

60   More recently, Aretxabaleta et al. (2014) analyzed water level data in Barnegat Bay and Great South Bay before and after Hurricane Sandy and demonstrated that the offshore-bay transfer was not significantly altered by the geomorphologic changes caused by the storm. Aretxabaleta et al. (2017) described observed changes in both tidal amplitude and bay water level transfer from offshore in Great South Bay and connected bays and related the changes to the dredging of nearby inlets and the changing size of a breach across Fire Island caused by Hurricane Sandy. They also introduced an analytical model,

65   based on the Chuang and Swenson (1981) approach but extended to interconnected bays, that incorporated bay and inlet dimensions and matched the observed transfer of offshore water level fluctuations into the bay system.

In this study, we combine an analysis of observed water levels in Barnegat Bay with the results of numerical models and an analytical description of the system to characterize the spatial characteristics of the bay response to offshore fluctuations. The observations provide detailed information at five locations in the bay, while the numerical simulations can expand the

70   analysis to the entire bay system. The analytical model allows for the evaluation of the importance of the dominant factors affecting water level in bays. The combined approach can be used to provide consistent spatial maps of offshore water level impact into back-barrier bays. The method will be useful for coastal hazard assessment assisting in the management of nuisance flooding (Moftakhari et al., 2018) and providing spatial differences in vulnerability to perigean spring tides (king tides) and planning for flooding in response to storms of different durations. The final hazard estimates will be included as

2

Alfredo Lopez de Are…, 4/3/2019 3:37 PM
**Deleted:** smaller

part of the U.S. Geological Survey Coastal Change Hazard portal (USGS, 2018) in the effort to expand the total water level predictions (Aretxabaleta et al., 2019).

## 2. Regional description

The Barnegat Bay-Little Egg Harbor (BBLEH) estuary is a back-barrier bay along the coast of New Jersey (Figure 1). It is a shallow (average depth around 1.5 m) bay connected to the ocean through three openings: Little Egg Inlet in the south, Barnegat Inlet in the center, and Point Pleasant Canal, a much smaller connection in the north of the bay. Offshore tidal amplitudes decrease slightly from 0.7 m in northern New York Bay to 0.6 m in central New Jersey. The southern sub-embayment (Little Egg Harbor) is more connected with the open ocean with tidal amplitudes ranging between 0.2 and 0.5 m, while the northern part (Barnegat Bay) has less exchange and tidal amplitudes are smaller than 0.2 m (Chant, 2001; Defne and Ganju, 2015).

## 3. Observational and model data

Water level observations from five stations in the BBLEH system (Table 1) and from two external coastal stations are used to determine transfer from ocean to bay. The bay stations started recording in October 2007, while Sandy Hook and Atlantic City are long-term NOAA water level stations operational since 1910 and 1911, respectively (Table 1). Wind observations were obtained from the NDBC buoy 44065 (New York Harbor Entrance) for the period 2008-2018.

We used numerical simulations of Barnegat Bay for the period March-September 2012 (Defne and Ganju, 2015) and October-December 2012 (Defne and Ganju, 2019) to obtain the spatial character of the water level response. The simulations used the Coupled Ocean Atmospheric Wave Sediment Transport modeling system (COAWST; Warner et al., 2010). The model resolution ranged from 40 m to 200 m, with the higher resolution located near complex geometry and around the inlets. The model is forced at the boundaries with tides from the ADCIRC tidal database for the western North Atlantic Ocean (Szpilka et al., 2016) and open-ocean forcing from subtidal water level and velocity from the ESPreSSO model (Wilkin and Hunter, 2013; http://www.myroms.org/espresso/) and COAWST US east coast forecast (Warner et al., 2010; https://catalog.data.gov/dataset/coawst-forecast-system-usgs-us-east-coast-and-gulf-of-mexico-experimentalf9168). Defne and Ganju (2015) showed the numerical model solution had sufficient flow and elevation skill to characterize bay dynamics under normal and storm conditions.

The impact in the bay of offshore forcing can be evaluated spectrally by estimating transfer functions in frequency space between observed water levels offshore (input) and in the bays (output). The transfer functions are calculated using a Hanning window with over-lapping (50%) data segments with a length of 29 days to provide estimates near the main tidal frequencies (Aretxabaleta et al., 2017). The uncertainty envelopes for the transfer function are estimated using the Bendat and Piersol (1986) formulation.

3

Alfredo Lopez de Ar…, 5/31/2019 9:52 PM
**Deleted:** –

Alfredo Lopez de Ar…, 5/31/2019 9:52 PM
**Deleted:** which is

Alfredo Lopez de Ar…, 5/31/2019 9:52 PM
**Deleted:** 1

**4 Analytical Water Level Models**

110 **4.1 Offshore Impact on Bay Model**

The impact of ocean sea level fluctuations in the bay can be explored with an analytical model of a generic bay system (Figure 2) consisting of multiple interconnected sub-embayments connected to the offshore by three separate inlets: Little Egg Inlet, Barnegat Inlet, and Point Pleasant Canal. The model assumes that the bay water level responds as a level surface in each sub-embayment to ocean fluctuations, as local forcing in the bay is not included. The formulation is an extension of

115 the approach proposed by Chuang and Swenson (1981) for a single inlet connecting to a bay and expanded by Wong and DiLorenzo (1988) to two connected bays and to multiple bays and inlets by Aretxabaleta et al. (2017). An analytical solution can be found for the entire system with expressions for all the connections in the system. The model solves the along-channel depth-averaged momentum equation based on the balance between frictional effects and the elevation gradient between offshore and bay and the continuity equation for the bay/channel system based on the changing volume of the bays

120 as water flows through the inlets. The model also allows the estimation of the effect of the breach in Mantoloking during Hurricane Sandy. An analytical solution can be found by dividing the entire system into 5 sub-embayments (based on constrictions inside the bay system) resulting in a system of equations that includes 13 equations and unknowns (Appendix A).

$$
\frac{\partial}{\partial t}\begin{pmatrix} u_1 \\ u_2 \\ u_3 \\ u_4 \\ u_5 \\ u_6 \\ u_7 \\ u_8 \end{pmatrix} = g \begin{pmatrix} 1/L_1 \\ 1/L_2 \\ 1/L_3 \\ 1/L_4 \\ 1/L_5 \\ 1/L_6 \\ 1/L_7 \\ 1/L_8 \end{pmatrix} \begin{pmatrix} \eta_o \phi_{LEI} - \eta_1 \\ \eta_1 - \eta_2 \\ \eta_2 - \eta_3 \\ \eta_o \phi_{BI} - \eta_3 \\ \eta_3 - \eta_4 \\ \eta_4 - \eta_5 \\ \eta_o \phi_{breach} - \eta_5 \\ \eta_o \phi_{PPC} - \eta_5 \end{pmatrix} - \begin{pmatrix} u_1 r_1/h_1 \\ u_2 r_2/h_2 \\ u_3 r_3/h_3 \\ u_4 r_4/h_4 \\ u_5 r_5/h_5 \\ u_6 r_6/h_6 \\ u_7 r_7/h_7 \\ u_8 r_8/h_8 \end{pmatrix} \qquad (1)
$$

$$
\begin{pmatrix} A_1 \\ A_2 \\ A_3 \\ A_4 \\ A_5 \end{pmatrix} \frac{\partial}{\partial t}\begin{pmatrix} \eta_1 \\ \eta_2 \\ \eta_3 \\ \eta_4 \\ \eta_5 \end{pmatrix} = \begin{pmatrix} h_1 W_1 u_1 - h_2 W_2 u_2 \\ h_2 W_2 u_2 - h_3 W_3 u_3 \\ h_3 W_3 u_3 + h_4 W_4 u_4 - h_5 W_5 u_5 \\ h_5 W_5 u_5 - h_6 W_6 u_6 \\ h_6 W_6 u_6 + h_7 W_7 u_7 + h_8 W_8 u_8 \end{pmatrix} \qquad (2)
$$

4

where $g$ is the gravitational acceleration, $A_m$ is the surface area of sub-embayment $m$; $\eta_m$ the sea level in the $m$ sub-embayment; $\eta_o$ the sea level in the ocean; with $h_n$ the water depth; $W_n$ the width; $L_n$ the length, and $r_n$ the linear drag coefficient of channel $n$. $\phi_{LEI}, \phi_{BI}, \phi_{breach}, \phi_{PPC}$ are the <u>linear frequency-dependent</u> relationships between the water levels at offshore proxy stations (Sandy Hook or Atlantic City) and the water level just offshore of Little Egg Inlet, Barnegat Inlet, the breach at Mantoloking caused by Sandy, and Point Pleasant Canal.

Assuming $\eta = \tilde{\eta} e^{i\omega t}$ and $u = \tilde{u} e^{i\omega t}$ where $\tilde{\eta}$ and $\tilde{u}$, represent the magnitude of the water level and velocity oscillations, respectively. TThen we can define $K_n = \dfrac{h_n W_n g}{L_n\left(\frac{r_n}{h_n}+i\omega\right)}$ for $n$=1,…, 8

then with the proper rearrangement, it yields:

$$\widetilde{\eta_3} = \frac{K_4\eta_o\phi_{BI} + \cfrac{\cfrac{K_1 K_2 K_3 \widetilde{\eta_o}\phi_{LEI}}{i\omega A_1 + K_1 + K_2}}{i\omega A_2 + K_2 + K_3 - \cfrac{K_2 K_2}{i\omega A_1 + K_1 + K_2}} + \cfrac{\cfrac{K_5 K_6(K_7\phi_{breach} + K_8\phi_{PPC})\widetilde{\eta_o}}{i\omega A_5 + K_6 + K_7 + K_8}}{i\omega A_4 + K_5 + K_6 - \cfrac{K_6 K_6}{i\omega A_5 + K_6 + K_7 + K_8}}}{i\omega A_3 + K_3 + K_4 + K_5 - \cfrac{K_3 K_3}{i\omega A_2 + K_2 + K_3 - \cfrac{K_2 K_2}{i\omega A_1 + K_1 + K_2}} - \cfrac{K_5 K_5}{i\omega A_4 + K_5 + K_6 - \cfrac{K_6 K_6}{i\omega A_5 + K_6 + K_7 + K_8}}}$$

$$(3)$$

The solution for the water level of the central sub-embayment can be used to recursively calculate the solutions for the rest of the sub-embayments:

$$\widetilde{\eta_2} = \frac{K_3\widetilde{\eta_3} + \cfrac{K_2 K_1 \widetilde{\eta_o}\phi_{LEI}}{i\omega A_1 + K_1 + K_2}}{i\omega A_2 + K_2 + K_3 - \cfrac{K_2 K_2}{i\omega A_1 + K_1 + K_2}} \qquad (4)$$

$$\widetilde{\eta_4} = \frac{K_5\widetilde{\eta_3} + \cfrac{K_6(K_7\phi_{breach} + K_8\phi_{PPC})\widetilde{\eta_o}}{i\omega A_5 + K_6 + K_7 + K_8}}{i\omega A_4 + K_5 + K_6 - \cfrac{K_6 K_6}{i\omega A_5 + K_6 + K_7 + K_8}} \qquad (5)$$

$$\widetilde{\eta_1} = \frac{K_1\widetilde{\eta_o}\phi_{LEI} + K_2\widetilde{\eta_2}}{i\omega A_1 + K_1 + K_2} \qquad (6)$$

$$\widetilde{\eta_5} = \frac{(K_7\phi_{breach} + K_8\phi_{PPC})\widetilde{\eta_o} + K_6\widetilde{\eta_4}}{i\omega A_5 + K_6 + K_7 + K_8} \qquad (7)$$

The resulting expressions include all the sub-embayment and offshore exchanges under the same assumptions of the Chuang and Swenson (1981) model (e.g., no local influences, no overtopping).

5

## 4.2 Local Wind Impact on Bay Model

The contribution of local wind setup to the spatial distribution of water level inside the bay can be approximated following Wong and Moses-Hall (1998). The bay can be assumed to be a simple long well-mixed embayment for which the cross-bay gradients and vertical stratification can be ignored. The linearized vertically integrated momentum and mass conservation equations are:

$$\frac{\partial U}{\partial t} = -gh\frac{\partial \eta}{\partial x} + \frac{1}{\rho_0}(\tau_s - \tau_b) = -gh\frac{\partial \eta}{\partial x} + \tau_w - r\frac{U}{h} \qquad (8)$$

and

$$\frac{\partial U}{\partial x} = -\frac{\partial \eta}{\partial t} \qquad (99)$$

where $\eta$ is the water level in the bay; $U$ is the depth integrated along-bay velocity; $h$ is the water depth; $\tau_s$ and $\tau_b$ are the surface and bottom <u>dynamic</u> stresses, respectively; and $\rho_0$ is the water density. $\tau_w = \tau_s/\rho_0$ is the spatially invariant <u>kinematic</u> wind stress and $r$ is a linearized bottom friction.

Under the assumption of $\eta = \tilde{\eta}e^{i\omega t}$ and $u = \tilde{u}e^{i\omega t}$, where $\omega$ is the <u>cyclic (angular)</u> frequency, the resulting equation is:

$$\frac{\partial^2 \tilde{\eta}}{\partial x^2} + \tilde{\eta}\left(\frac{\omega^2}{gh} - \frac{i\omega r}{gh^2}\right) = \frac{\partial^2 \tilde{\eta}}{\partial x^2} + \tilde{\eta}k^2 = 0 \qquad (10)$$

with boundary conditions $\eta(x = 0, \omega) = 0$ assuming no offshore forcing at the entrance (this assumption will be revisited in the next section) and $\frac{\partial \tilde{\eta}\eta(x=L,\omega)}{\partial x} = \frac{\widetilde{\tau_w}\tau_w(\omega)}{gh}$ assuming no flux at the head ($x=L$). $\widetilde{\tau_w}(\omega)$ <u>represents the magnitude of the kinematic wind stress that results in water level fluctuations at a specific frequency.</u>

The solution is:

$$\tilde{\eta}(\omega) = \frac{\widetilde{\tau_w}\tau_w(\omega)\sin(kx)}{ghk\,\cos(LkLx)} \qquad (11)$$

where $k = \left(\frac{\omega^2}{gh} - \frac{i\omega r}{gh^2}\right)^{1/2}$. $\qquad (12)$

## 4.3 Combining Local and Remote Effects

The local and remote effects can be combined in following the approach by Wong and Moses-Hall (1998). The boundary condition for the local wind effect can be altered to account for the influence of offshore water level, $\eta_o$. The resulting model is a modification of the wind effect model that considers the analytical offshore influence in Section 4.1. In a system with a single inlet, the solution can be simply stated as in Wong and Moses-Hall (1998):

$$\tilde{\eta}(\omega) = \frac{\widetilde{\tau_w}\tau_w(\omega)\sin(kx)}{ghk\,\cos(kLx)} + \widetilde{\eta_0}(\omega)\frac{\cos(k(L-x))}{\cos(kLx)} \qquad (1)$$

In a system with multiple connections with the offshore, the solution can be more complex. One limitation of the approach is that it utilizes a linear friction approximation. To produce a better approximation that takes into account the complex

6

frictional conditions of the bay (e.g., varying geometry, diverse bottom conditions, enhanced attenuation over submerged vegetation), we can take a numerical solution of the bay that resolves the tidal and sub-tidal water level conditions under realistic friction and adjust the spatial distribution of the transfer from offshore accordingly. As most of the water level variability in the bay is associated with the $M_2$ semidiurnal tidal constituent (Figure 3) and the distribution of the tide

has been properly validated in the numerical simulations (Defne and Ganju, 2015), we can take the spatial distribution of the $M_2$ tidal amplitudeamplitude as a proxy for the internal frictional effects in the bay. Bottom friction caused by both wind driven and tidal effects is considered in the numerical simulations. By adjusting the water level based on the numerical $M_2$ spatial distribution, we are approximating the complete frictional characteristics of the bay. The adjustment is applied to each of the sub-embayments following the expression:

$$\frac{\hat{\eta}_j}{\eta_o}(x,\omega) = 1 - \frac{\left(1-\frac{\eta_j}{\eta_o}(\omega)\right)\left(1-\frac{\eta\,\eta_{M_2}\left(x,\omega_{M_2}\right)}{\eta\eta_{M_2}\left(offshore,\omega_{M_2}\right)}\right)}{\left(1-\frac{\eta_j}{\eta_o}\left(\omega_{M_2}\right)\right)} \qquad (1313)$$

where $\frac{\eta_j}{\eta_o}(\omega)$ is the transfer coefficient of the sub-embayment $i$ (single value) at frequency $\omega$, $\eta\left(x,\omega_{M_2}\right)$ is the amplitude of the $M_2$ tidal fluctuations from the numerical model solution (spatially variable), and $\frac{\hat{\eta}_j}{\eta_o}(x,\omega)$ is the spatially variable adjusted transfer coefficient for sub-embayment $j$. The resulting adjusted transfer coefficients provide

estimates of the spatial changes not only between adjacent sub-embayments but also inside each of the sub-embayments. The local wind effects on bay water level can be added to the impact from offshore fluctuations to obtain a combined local and remote water level response estimate.

**5 Results**

**5.1 Offshore transfer to bay**

The maximum energy in water level spectra (Figure 3, Table 2) was associated with the $M_2$ semidiurnal tidal constituent for the offshore proxies (SH and AC) and at the stations TUC and ETH in the southern part of the BBLEH area. For the locations in Barnegat Bay (WAR, SEH, MAN), maximum energy was in the low frequency band. Large spectral energy also occurred in the other semidiurnal tidal frequencies ($S_2$ and $N_2$), the diurnal frequencies ($O_1$ and $K_1$), the storm band (periods between 2 and 5 days), and the low frequency band (Table 2). The energy in the remaining bands exhibited average fluctuations less than 0.03 m in size offshore, while in the bay fluctuations were less than 0.01 m.

Transfer functions between Atlantic City (AC) and the five stations inside the bay (Figure 4) for the longest available length of record showed a north to south gradient. The transfer of the offshore fluctuations was 50-80% at periods between 2 and 5 days (storm band) except at Tuckerton (TUC; over 95%). The transfers at diurnal periods were about 35% for the three Barnegat Bay stations (WAR, SEH, MAN), about 45% in Little Egg Harbor (ETH), and 80% in Great Bay (TUC). For

7

250 frequencies associated with the semidiurnal tides, the transfers were even more attenuated with values about 15% (between 14 and 16%) inside Barnegat, 30-35% at ETH, and 60-70% at TUC. As the numerical model solution was only available for the period March-December 2012, the long-term (2007-2018) transfers were compared with shorter-term observations. The transfers were similar (within the uncertainty envelopes for each station, not shown) for both datasets at most frequencies except at Mantoloking (MAN) that showed enhanced transfers for periods between one and five days in the 2012 record and

255 at Seaside Heights (SEH), where transfers in the storm band were slightly attenuated during 2012. Transfer estimates using Sandy Hook (SH) as the offshore proxy instead of Atlantic City produced similar results (not shown). The transfer between stations AC and SH on the open coast (proxies for offshore fluctuations) has been shown to be close to one (Wong and Wilson, 1984; Aretxabaleta et al., 2014), confirming that the offshore forcing at all three inlets is about the same.

Transfers estimated from the numerical model solution (Figure 5) showed similar magnitudes to the observed transfers

260 (within uncertainty envelopes provided by the Bendat and Piersol (1986) formulation) at most frequencies. The observed and modeled transfer at diurnal and semi-diurnal transfers were similar (within a few percentage points) at all stations except the model overestimated the semidiurnal transfer at TUC. Differences between model and observed estimates at MAN and SEH only were significant at frequencies that contained minimal energy. The model reproduced the enhanced transfer in the storm band at Mantoloking during 2012, suggesting a physical mechanism for the change that the model was able to capture but

265 remains unexplained. The likely explanation is that the location of the Azores-Bermuda high-pressure system over the Atlantic in 2012 (Mattingly et al., 2012), associated with the negative phase of the North Atlantic Oscillation, resulted in average winds that lined up with the axis of the Bay and caused enhanced wind setup in the northern part of the bay. The model overestimated the transfer at ETH in the storm band and underestimated the low-frequency transfer at Waretown. The likely cause for some of the discrepancies, especially at low frequencies, is the relatively short length of the available record.

270 The analytical model of offshore impact that considered five sub-embayments (Section 4.1) was fit to the observed transfers to obtain an estimate of linear friction. The fit considered the unevenly distributed energy spectra (Figure 3) with adjusted weight to the semidiurnal and low-frequency components. The resulting friction was r = 0.021 m/s. The associated frictional adjustment time, $t_{fr} = {}^h/_r$, was about 1-5 minutes depending on the depth of the inlet. The analytical curves (Figure 6) matched the observed transfer function shape at most frequencies. The analytical model with five sub-embayment domains

275 captured the north-south spatial differences in transfer. The analytical model for the central Barnegat Bay sub-embayment ($A_3$) approximated the transfer estimates from observations at Waretown at most frequencies (less than 5 % in the storm band). The analytical model for Great Bay ($A_1$) adequately matched observed transfers at Tuckerton at diurnal and semidiurnal frequencies (less than 5 % difference) but underestimated the transfer in the storm band (model estimates about 90%, while observations were above 95%). Meanwhile, the analytical model for Little Egg Harbor (A2) matched the

280 observed transfers at ETH within the uncertainty envelope, except for a slight under-prediction at diurnal frequencies (less than 5%). The observed transfers at the northern stations (MAN and SEH) were reproduced by the analytical model ($A_4$, $A_5$ respectively) at diurnal and semidiurnal tides, but were under-predicted for the higher storm band frequencies (5-10% less transfer in frequencies close to 2-day periods) and over-predicted at low frequencies (about 10% differences). The analytical

8

model was used to explore the effect on transfer of the breach ($U_7$) at Mantoloking that opened during Hurricane Sandy. The transfers were so minimally affected that the curves are indistinguishable with only a negligible enhancement (<0.2%) in transfer in the northern most sub-embayment ($A_5$). The breach was too small and shallow for any significant volume transport to occur that would affect the large bay.

## 5.2 Local Wind Influence

The spectrum of the along-bay component (rotated 20 degrees) of the wind (Figure 7a) from the offshore buoy NDBC 44065 (ten years, 2008-2018) showed high energies in the storm band (2-5 days) and in low frequencies. The largest single peak of energy was associated with 24-hour period oscillations likely associated with sea breeze and matched energy values at 5-day frequencies. There was a small peak at inertial frequencies.

The local wind contribution to water level setup inside the bay was approximated using the Wong and Moses-Hall (1998) approach (Section 4.2). The resulting formulation showed largest setup magnitudes near the head of the bay (e.g., northern part with wind blowing from the south) with a decay as distance from head increased (Figure 7b,c). The magnitude of the setup depended on the magnitude of the linear friction with less setup under stronger friction (Figure 7b,c). The setup responded exponentially to fetch (distance) except under long duration and low friction conditions, which was predominantly linear (Figure 7b). The frictional control was less important at higher frequencies (Figure 7c). As frequency increased there was less wind energy (Figure 7a), so the frictional control is mostly important for low frequency and storm band fluctuations.

The resulting effect of the wind setup (or set-down) was small (less than 0.1 m with an along-bay wind stress of 0.1 Pa) for most of the domain (Figure 8). The estimate assumed a linear friction of the same magnitude as in Section 5.1 ($r$=0.021 m/s). Under persistent wind stress of 0.1 Pa (about 8 m/s wind speed) in the along-bay direction, the resulting setups varied depending on the frequency considered. Setup magnitudes over 0.22 m were estimated for the 5-day period wind (Figure 8c), while under half of that magnitude was achieved for the 2-day persistent wind (Figure 8b), and much smaller water level setup (peak smaller than 0.1 m) was estimated for the sea breeze (Figure 8a). During extreme events like Hurricane Sandy, under intense wind stress, two additional effects should be considered: the depth of the bay increases by the transfer of offshore surge resulting in altered setup response (Section 4.2), and the frictional effect is enhanced (a larger linear friction would be needed) by the presence of wave-induced roughness.

## 6 Discussion

### 6.1 Spatially Variable Water Level Transfer

Following the approach described in Section 4.3, estimates of spatially variable water level impact from offshore can be calculated (Figure 9). The $M_2$ tidal constituent transfer (Figure 9a) showed a large north to south gradient with values going

9

from around 10% in the north to over 80% in the vicinity of Little Egg Inlet. The role of Barnegat Inlet in enhancing tidal transfer was greatly reduced as most of the tide was attenuated in the inlet. The contribution of Point Pleasant Canal was also small as expected from the tidal amplitudes (Chant, 2001; Defne and Ganju, 2015). The transfer in the storm band of 2-day fluctuations (Figure 9b) also showed a strong north-south gradient with values about 50% in Barnegat Bay, around 70-80% in Little Egg Harbor and larger values in Great Bay. The 5-day offshore fluctuations were transferred more efficiently into the bay (Figure 9c) with values over 70% in the entire bay, reaching 80-90% in Little Egg Harbor, and over 90% in Great Bay. Both storm band transfer estimates were controlled by the exchange through Little Egg Inlet, with very local transfer enhancements in the vicinity of Barnegat Inlet and Point Pleasant Canal. While the presented estimates used Atlantic City as offshore proxy, similar results were obtained when Sandy Hook was used as the offshore reference (as expected from Aretxabaleta et al., 2014).

When the magnitude of the fluctuations associated with a specific storm are available $\eta_o$, then an estimate of the average water level in the bay during the storm can be obtained. For instance, for Hurricane Sandy the offshore surge associated with the storm was of the order of 2-3 m. Considering that the storm lasted for over a day, the water level transfer would have been above 50% in Barnegat Bay and above 70% in Little Egg Harbor. The resulting surge estimate in the bay was between 1 and 2 m just considering the exchange through the existing inlets. There was reported overtopping of the barrier island during the storm (McKenna et al., 2016) that might have further increased water level in the bay that the proposed method does not consider.

The wind setup effect inside the bay due to local wind can also be estimated for Hurricane Sandy using the approach in Section 4.2. Maximum wind stress during the storm was about 1 Pa. To obtain a maximum effect (worst-case scenario) the wind was assumed to be persistently in the along-bay direction and that maximum stress was maintained for the duration of the storm. The maximum resulting water level considering the Wong and Moses-Hall method is linear with regard to wind stress magnitude (Figure 7b) and would have been 10 times larger than the setup in Figure 8b. The maximum wind setup would have been between 1 and 2 m, which was of the same order of magnitude as the surge produced from offshore sources. The cross-bay contribution to the wind setup during Sandy was comparatively small as wind direction was predominantly along-bay. Surge estimates from simple analytical formulations (State Committee for the Zuiderzee, 1926; Pugh, 1987) that do not consider storm duration produce similar magnitude results and are also dependent on the frictional response of the bay.

### 6.2 Transfer Based on Tidal Database

The approach thus far was based on the combination of observations, analytical models, and numerical models. In many systems, long-term observations that allow for the estimation of transfer coefficients might not be available. Also, numerical solutions of back-barrier bay systems tend to be computationally expensive and might not be available for the period of interest. We propose a relatively simpler approach for some of these systems based on the availability of high-resolution

10

tidal solutions for the system. The EC2015 ADCIRC tidal database (Szpilka et al., 2016) showed sufficient resolution (down to 13m in some areas) in many bays along the east coast of the United States to resolve the tidal conditions with skill when compared to NOAA CO-OPS stations and historic International Hydrographic Organization (IHO) data. The EC2015 tidal database provides estimates for 37 tidal constituents. Based on those constituents and assuming that the totality of the

365 offshore fluctuations at zero frequency reach the interior of the bay, an estimate can be provided for the storm band frequencies. A weighted least squares interpolation in the frequency domain was performed based on the $M_4$, $K_2$, $S_2$, $L_2$, $M_2$, $N_2$, $K_1$, $P_1$, $O_1$, $Q_1$ tidal amplitudes ratios between each point of the ADCIRC domain inside the bay and a point in the offshore. Higher weight was given to zero frequency to nudge toward 100% transfer at zero frequency. Estimates were calculated based on multiple locations inside the bay and average to achieve a more robust calculation and also obtain an

370 approximation to the uncertainty associated with the estimate.

The resulting transfer estimates (Figure 10) exhibited the same general spatial patterns shown in the previous estimates (Figure 9) with slight differences. Some of the smaller features present in the COAWST numerical solution (Defne and Ganju, 2015) were not present in the ADCIRC EC2015 domain. The $M_2$ transfer estimate based on the tidal database (Figure 10a) presented approximately the same magnitudes in most areas (average difference less than 3%). The 5-day transfer

375 (Figure 10c) was also comparable to the solution described in Section 6.1 with values over 70% in the entire domain and the southern areas exceeding 90% transfer. The 2-day transfer from ADCIRC (Figure 10b) was 5-10% higher than the direct estimates (Figure 9b). One of the benefits of the ADCIRC approach was the possibility of providing an approximation to the uncertainty (Figure 11). The uncertainty estimate of the $M_2$ transfer was about 1-2% (Figure 11a) with higher values in the southern part of the domain. The 2-day transfer uncertainty (Figure 11b) was above 4% in Barnegat Bay in areas of larger

380 discrepancy between the ADCIRC and complete approaches. The uncertainty estimates in the 5-day offshore water level transfer (Figure 11c) in the northern part of the domain did not exceed 2.5%.

The magnitude of the difference between the ADCIRC tidal database approach and the complete method highlighted in Section 4.3 was of the same order of magnitude or even smaller than the difference between observations and analytical model (Figure 6) or between observed and numerical modeled transfers (Figure 5). This result emphasizes the validity of

385 using the tidal database to calculate offshore transfer estimates, especially when water level observations inside the bay or numerical solutions are not available.

The effect of local wind setup will also need to be added to the ADCIRC-based estimate, especially during severe storms. The approach discussed in Section 5.2 or even a simpler surge calculation (e.g., from the steady state vertically averaged momentum equations, as in Pugh (1987), from the traditional report of the State Committee for the Zuiderzee (1926), or the

390 updated frequency domain equivalent from Reef et al., 2018) could be used and the resulting elevation could be added to the offshore transfer estimate obtain based on the ADCIRC tides. Thus, the production of bay water level predictions will require accurate wind forecast products.

11

**6.3 Validity for Flooding Hazard Assessments**

The method presented offers a new methodology for coastal hazards assessment and risk analysis. While many
395  methodologies are being used for open-coast regions (Thieler and Hammar-Klose, 1999; Kunreuther et al., 2000),
vulnerability evaluation to coastal hazards in back-barrier bays remains under developed. Evaluating bay hazards usually
requires expensive computational simulations at appropriate high resolutions to characterize the spatial and temporal effects.
The method presented here, using existing ADCIRC results, provides a less expensive approach that is able to properly
estimate the spatial differences in vulnerability in response to flooding at different time scales (e.g., perigean spring tides,
400  storms of different duration). It provides guidance for planning in response to "nuisance" flooding at a relatively low cost. It
can be expanded to all back-barriers without the need to simulate each storm in each embayment, while applying a consistent
methodology.

Careful consideration needs to be given to the estimation of coastal hazards especially for the forecast of intense storm
effects. The inclusion of meticulously validated methodologies that consider both offshore influences (e.g., using the transfer
405  estimated from ADCIRC tides) and local wind setup (e.g., Wong and Moses-Hall, 1998; Reef et al., 2018) is necessary. Skill
assessment of storm hazard estimates using adequate observations is critical to avoid producing under- or over-predictions of
flooding and inundation.

As part of the general needs for hazard assessment (Ludwig et al., 2018), the important hazard characteristics that decision
makers require include spatial extent, duration, and magnitude. The proposed methodology provides an approximation to
410  both the area extent and magnitude, and also variations based on storm duration. Additionally, the fact that uncertainty
estimates accompany the vulnerability provided by the present method enhances the potential value to decision makers. The
extension to other bays in the United States will be included as part of the U. S. Geological Survey Coastal Change Hazards
portal (USGS, 2018).

**7 Summary**

415  The results presented here demonstrate a strategy for estimating the impact of offshore sea level and local wind setup in
back-barrier bay water levels. The transfer estimates of offshore to bay water level used a combination of observations,
analytical models based on appropriate simplifications of the bay system, and numerical simulations that provide the needed
spatial distribution and more realistic frictional control.

The resulting maps of water level response to offshore forcing showed larger attenuation of the relatively higher frequency
420  fluctuations such as the semidiurnal tides. Smaller transfers were associated with shorter duration storms than longer
duration storms and transfer was most spatially uniform for storms of long duration.  The description of the magnitude and
spatial dependence of transfer on storm duration will assist planning for flooding in back-barrier bays.

12

In the specific case of the Barnegat Bay-Little Egg Harbor system, larger transfers were estimated for the southern embayments (Great Bay and Little Egg Harbor) when compared to Barnegat Bay. The reason for the difference was the dominant role of Little Egg Inlet (wider and deeper) in controlling the exchange between the offshore and bay systems. During relatively small storms, the contribution of local wind to bay water level setup was smaller than the transfer from offshore fluctuations. During intense events, like hurricanes, local wind setup was of the same order of magnitude or even larger than offshore influences depending on wind magnitude and especially the relative angle of the wind with respect to bay orientation.

We introduced two approaches depending on the availability of observations and numerical solutions. The less data-requiring approach based on the ADCIRC tidal database provides spatial offshore transfer estimates and measures of uncertainty. In both cases, the inclusion of the local wind setup could be achieved based on simple surge analytical estimates. The approach that includes an analytical model allows for a simple tool to study the response of back-barrier bay systems to alternative conditions and forcing (e.g., geomorphic changes, changing duration of storms, sea level rise).

The proposed method represents an effective and inexpensive approach to flooding hazard evaluation in back-barrier bays and inland waters. The method provides detailed spatial estimates of vulnerabilities and uncertainties that could be an intuitive tool for coastal managers.

**Appendix A**

The offshore impact in the bays water level can be approximated with an analytical model that solves the linearized depth-averaged momentum equations. The system of equations for an idealized simplification of Barnegat Bay (Figure 2) that includes 5 sub-embayments (based on constrictions inside the bay system) consists of 13 equations and unknowns.

$$\frac{\partial}{\partial t}\begin{pmatrix} u_1 \\ u_2 \\ u_3 \\ u_4 \\ u_5 \\ u_6 \\ u_7 \\ u_8 \end{pmatrix} = g \begin{pmatrix} 1/L_1 \\ 1/L_2 \\ 1/L_3 \\ 1/L_4 \\ 1/L_5 \\ 1/L_6 \\ 1/L_7 \\ 1/L_8 \end{pmatrix} \begin{pmatrix} \eta_o\phi_{LEI} - \eta_1 \\ \eta_1 - \eta_2 \\ \eta_2 - \eta_3 \\ \eta_o\phi_{BI} - \eta_3 \\ \eta_3 - \eta_4 \\ \eta_4 - \eta_5 \\ \eta_o\phi_{breach} - \eta_5 \\ \eta_o\phi_{PPC} - \eta_5 \end{pmatrix} - \begin{pmatrix} u_1 r_1/h_1 \\ u_2 r_2/h_2 \\ u_3 r_3/h_3 \\ u_4 r_4/h_4 \\ u_5 r_5/h_5 \\ u_6 r_6/h_6 \\ u_7 r_7/h_7 \\ u_8 r_8/h_8 \end{pmatrix} \qquad \text{(A1)}$$

13

$$\begin{pmatrix} A_1 \\ A_2 \\ A_3 \\ A_4 \\ A_5 \end{pmatrix} \frac{\partial}{\partial t} \begin{pmatrix} \eta_1 \\ \eta_2 \\ \eta_3 \\ \eta_4 \\ \eta_5 \end{pmatrix} = \begin{pmatrix} h_1 W_1 u_1 - h_2 W_2 u_2 \\ h_2 W_2 u_2 - h_3 W_3 u_3 \\ h_3 W_3 u_3 + h_4 W_4 u_4 - h_5 W_5 u_5 \\ h_5 W_5 u_5 - h_6 W_6 u_6 \\ h_6 W_6 u_6 + h_7 W_7 u_7 + h_8 W_8 u_8 \end{pmatrix} \quad\text{(2)}$$

$\phi_{LEI}, \phi_{BI}, \phi_{breach}, \phi_{PPC}$ are linear frequency-dependent relationships between the water levels at offshore proxy stations (Sandy Hook or Atlantic City) and the water level just offshore of Little Egg Inlet, Barnegat Inlet, the breach at Mantoloking caused by Sandy, and Point Pleasant Canal.

By performing Fourier transforms on the momentum equations ($\eta = \tilde{\eta} e^{i\omega t}$ and $u = \tilde{u} e^{i\omega t}$, where $\tilde{\eta}$ and $\tilde{u}$, represent the magnitude of the water level and velocity oscillations, respectively), we obtain:

$$i\omega \begin{pmatrix} \widetilde{u}_1 \\ \widetilde{u}_2 \\ \widetilde{u}_3 \\ \widetilde{u}_4 \\ \widetilde{u}_5 \\ \widetilde{u}_6 \\ \widetilde{u}_7 \\ \widetilde{u}_8 \end{pmatrix} = g \begin{pmatrix} 1/L_1 \\ 1/L_2 \\ 1/L_3 \\ 1/L_4 \\ 1/L_5 \\ 1/L_6 \\ 1/L_7 \\ 1/L_8 \end{pmatrix} \begin{pmatrix} \widetilde{\eta}_o \phi_{LEI} - \widetilde{\eta}_1 \\ \widetilde{\eta}_1 - \widetilde{\eta}_2 \\ \widetilde{\eta}_2 - \widetilde{\eta}_3 \\ \widetilde{\eta}_o \phi_{BI} - \widetilde{\eta}_3 \\ \widetilde{\eta}_3 - \widetilde{\eta}_4 \\ \widetilde{\eta}_4 - \widetilde{\eta}_5 \\ \widetilde{\eta}_o \phi_{breach} - \widetilde{\eta}_5 \\ \widetilde{\eta}_o \phi_{PPC} - \widetilde{\eta}_5 \end{pmatrix} - \begin{pmatrix} \widetilde{u}_1 r_1 / h_1 \\ \widetilde{u}_2 r_2 / h_2 \\ \widetilde{u}_3 r_3 / h_3 \\ \widetilde{u}_4 r_4 / h_4 \\ \widetilde{u}_5 r_5 / h_5 \\ \widetilde{u}_6 r_6 / h_6 \\ \widetilde{u}_7 r_7 / h_7 \\ \widetilde{u}_8 r_8 / h_8 \end{pmatrix} \quad\text{(Ap3)}$$

and then:

14

$$
\begin{pmatrix} \widetilde{u_1} \\ \widetilde{u_2} \\ \widetilde{u_3} \\ \widetilde{u_4} \\ \widetilde{u_5} \\ \widetilde{u_6} \\ \widetilde{u_7} \\ \widetilde{u_8} \end{pmatrix} = g \begin{pmatrix} \widetilde{\eta}_o \phi_{LEI} - \widetilde{\eta}_1 \\ \widetilde{\eta}_1 - \widetilde{\eta}_2 \\ \widetilde{\eta}_2 - \widetilde{\eta}_3 \\ \widetilde{\eta}_o \phi_{BI} - \widetilde{\eta}_3 \\ \widetilde{\eta}_3 - \widetilde{\eta}_4 \\ \widetilde{\eta}_4 - \widetilde{\eta}_5 \\ \widetilde{\eta}_o \phi_{breach} - \widetilde{\eta}_5 \\ \widetilde{\eta}_o \phi_{PPC} - \widetilde{\eta}_5 \end{pmatrix} \Bigg/ \begin{pmatrix} L_1 \\ L_2 \\ L_3 \\ L_4 \\ L_5 \\ L_6 \\ L_7 \\ L_8 \end{pmatrix} \begin{bmatrix} \begin{pmatrix} i\omega + r_1/h_1 \\ i\omega + r_2/h_2 \\ i\omega + r_3/h_3 \\ i\omega + r_4/h_4 \\ i\omega + r_5/h_5 \\ i\omega + r_6/h_6 \\ i\omega + r_7/h_7 \\ i\omega + r_8/h_8 \end{pmatrix} \end{bmatrix} \qquad \text{(Ap4)}
$$

Performing the Fourier transform on the continuity equations (Eq. Ap2) and substituting the velocity values from Eq. Ap4, we obtain:

$$
i\omega \begin{pmatrix} A_1\,\widetilde{\eta_1} \\ A_2\,\widetilde{\eta_2} \\ A_3\,\widetilde{\eta_3} \\ A_4\,\widetilde{\eta_4} \\ A_5\,\widetilde{\eta_5} \end{pmatrix} =
$$

$$
g \begin{pmatrix} h_1 W_1 \left( \widetilde{\eta}_o \phi_{LEI} - \widetilde{\eta}_1 \right) \Big/ L_1 \left( i\omega + r_1/h_1 \right) - h_2 W_2 \left( \widetilde{\eta}_1 - \widetilde{\eta}_2 \right) \Big/ L_2 \left( i\omega + r_2/h_2 \right) \\[2mm] h_2 W_2 \left( \widetilde{\eta}_1 - \widetilde{\eta}_2 \right) \Big/ L_2 \left( i\omega + r_2/h_2 \right) - h_3 W_3 \left( \widetilde{\eta}_2 - \widetilde{\eta}_3 \right) \Big/ L_3 \left( i\omega + r_3/h_3 \right) \\[2mm] h_3 W_3 \left( \widetilde{\eta}_2 - \widetilde{\eta}_3 \right) \Big/ L_3 \left( i\omega + r_3/h_3 \right) + h_4 W_4 \left( \widetilde{\eta}_o \phi_{BI} - \widetilde{\eta}_3 \right) \Big/ L_4 \left( i\omega + r_4/h_4 \right) - h_5 W_5 \left( \widetilde{\eta}_3 - \widetilde{\eta}_4 \right) \Big/ L_5 \left( i\omega + r_5/h_5 \right) \\[2mm] h_5 W_5 \left( \widetilde{\eta}_3 - \widetilde{\eta}_4 \right) \Big/ L_5 \left( i\omega + r_5/h_5 \right) - h_6 W_6 \left( \widetilde{\eta}_4 - \widetilde{\eta}_5 \right) \Big/ L_6 \left( i\omega + r_6/h_6 \right) \\[2mm] h_6 W_6 \left( \widetilde{\eta}_4 - \widetilde{\eta}_5 \right) \Big/ L_6 \left( i\omega + r_6/h_6 \right) + h_7 W_7 \left( \widetilde{\eta}_o \phi_{breach} - \widetilde{\eta}_5 \right) \Big/ L_7 \left( i\omega + r_7/h_7 \right) + h_8 W_8 \left( \widetilde{\eta}_o \phi_{PPC} - \widetilde{\eta}_5 \right) \Big/ L_8 \left( i\omega + r_8/h_8 \right) \end{pmatrix}
$$

Then, we can define $K_n = \dfrac{h_n W_n g}{L_n \left( \frac{r_n}{h_n} + i\omega \right)}$ for each channel $n=1,\dots,8$ and with the proper rearrangement:

15

$$\left(\begin{array}{c} i\omega A_1\,\widetilde{\eta_1} = K_1\widetilde{\eta_o}\phi_{LEI} - K_1\widetilde{\eta_1} - K_2\widetilde{\eta_1} + K_2\widetilde{\eta_2} \\ i\omega A_2\,\widetilde{\eta_2} = K_2\widetilde{\eta_1} - K_2\widetilde{\eta_2} - K_3\widetilde{\eta_2} + K_3\widetilde{\eta_3} \\ i\omega A_3\,\widetilde{\eta_3} = K_3\widetilde{\eta_2} - K_3\widetilde{\eta_3} + K_4\widetilde{\eta_o}\phi_{BI} - K_4\widetilde{\eta_3} - K_5\widetilde{\eta_3} + K_5\widetilde{\eta_4} \\ i\omega A_4\,\widetilde{\eta_4} = K_5\widetilde{\eta_3} - K_5\widetilde{\eta_4} - K_6\widetilde{\eta_4} + K_6\widetilde{\eta_5} \\ i\omega A_5\,\widetilde{\eta_5} = K_6\widetilde{\eta_4} - K_6\widetilde{\eta_5} + K_7\widetilde{\eta_o}\phi_{breach} - K_7\widetilde{\eta_5} + K_8\widetilde{\eta_o}\phi_{PPC} - K_8\widetilde{\eta_5} \end{array}\right) \qquad (Ap6)$$

The system of equations can be solved by substitution.

$$\widetilde{\eta_5} = \frac{(K_7\phi_{breach} + K_8\phi_{PPC})\widetilde{\eta_o} + K_6\widetilde{\eta_4}}{i\omega A_5 + K_6 + K_7 + K_8} \qquad (Ap7)$$

$$\widetilde{\eta_4} = \frac{K_5\widetilde{\eta_3} + \frac{K_6(K_7\phi_{breach} + K_8\phi_{PPC})\widetilde{\eta_o}}{i\omega A_5 + K_6 + K_7 + K_8}}{i\omega A_4 + K_5 + K_6 - \frac{K_6 K_6}{i\omega A_5 + K_6 + K_7 + K_8}} \qquad (Ap8)$$

$$\widetilde{\eta_1} = \frac{K_1\widetilde{\eta_o}\phi_{LEI} + K_2\widetilde{\eta_2}}{i\omega A_1 + K_1 + K_2} \qquad (Ap9)$$

$$\widetilde{\eta_2} = \frac{K_3\widetilde{\eta_3} + \frac{K_2 K_1\widetilde{\eta_o}\phi_{LEI}}{i\omega A_1 + K_1 + K_2}}{i\omega A_2 + K_2 + K_3 - \frac{K_2 K_2}{i\omega A_1 + K_1 + K_2}} \qquad (Ap10)$$

and finally,

$$\widetilde{\eta_3} = \frac{K_4\eta_o\phi_{BI} + \dfrac{\dfrac{K_1 K_2 K_3\widetilde{\eta_o}\phi_{LEI}}{i\omega A_1 + K_1 + K_2}}{i\omega A_2 + K_2 + K_3 - \dfrac{K_2 K_2}{i\omega A_1 + K_1 + K_2}} + \dfrac{\dfrac{K_5 K_6(K_7\phi_{breach} + K_8\phi_{PPC})\widetilde{\eta_o}}{i\omega A_5 + K_6 + K_7 + K_8}}{i\omega A_4 + K_5 + K_6 - \dfrac{K_6 K_6}{i\omega A_5 + K_6 + K_7 + K_8}}}{i\omega A_3 + K_3 + K_4 + K_5 - \dfrac{K_3 K_3}{i\omega A_2 + K_2 + K_3 - \dfrac{K_2 K_2}{i\omega A_1 + K_1 + K_2}} - \dfrac{K_5 K_5}{i\omega A_4 + K_5 + K_6 - \dfrac{K_6 K_6}{i\omega A_5 + K_6 + K_7 + K_8}}}$$
$$(Ap11)$$

As it only depends on the offshore water level, the solution for the water level of the central sub-embayment (Ap11) can be used to recursively calculate the solutions for the rest of the sub-embayments by substituting into Equations Ap7, AP8, Ap9, and Ap10.

## Author Contribution

A.L. Aretxabaleta developed the methodology and wrote most of the manuscript. N.K. Ganju and R.P. Signell suggested improvements to the methodology. Z. Defne contributed to the figure generation, the COAWST simulation analysis, and the discussion of results. All authors contributed to the final version.

## Competing Interests

The authors declare that they have no conflict of interest.

**Disclaimer**

Use of firm and product names is for descriptive purposes only and does not imply endorsement by the U.S. Government.

**References**

Aretxabaleta, A. L., Butman, B., and Ganju, N. K.: Water level response in back-barrier bays unchanged following Hurricane Sandy, Geophys. Res. Lett., 41, 9, 3163–3171, doi:10.1002/2014GL059957, 2014.

495 Aretxabaleta, A. L., Ganju, N. K., Butman, B., and Signell, R. P.: Observations and a linear model of water level in an interconnected inlet- bay system, J. Geophys. Res., 122, doi:10.1002/2016JC012318, 2017.

Aretxabaleta, A. L., Doran, K. S., Long, J. W., Erikson, L., and Storlazzi, C. D.: Toward a national coastal hazard forecast of total water levels, In The Proceedings of the Coastal Sediments 2019, 1373-1384, 2019.

Bendat, J. S., and Piersol, A. G.: Random data. Analysis and measurement procedures, 566 pp., John Wiley & Sons, New

500 York, 1986.

Chant, R. J.: Tidal and subtidal motion in a shallow bar-built multiple inlet/bay system, J. Coast. Res., 32(Special Issue), 102-114, 2001.

Chuang, W.-S., and Swenson, E. M.: Subtidal Water level variations in Lake Pontchartrain, Louisiana, J. Geophys. Res., 86(C5), 4198–4204, doi:10.1029/JC086iC05p04198, 1981.

505 Defne, Z., and Ganju, N. K.: Quantifying the Residence Time and Flushing Characteristics of a Shallow, Back-Barrier Estuary: Application of Hydrodynamic and Particle Tracking Models, Estuaries and Coasts, 38, 1719–1734, doi: 10.1007/s12237-014-9885-3, 2015.

Defne, Z., and Ganju, N. K.: Collection of USGS Barnegat Bay hydrodynamic model simulations for Hurricane Sandy: U.S. Geological Survey data release, https://doi.org/10.5066/P99K85SW, 2019.

510 Garvine, R. W.: A simple model of estuarine subtidal fluctuations forced by local and remote wind stress, J. Geophys. Res., 90(C6), 11,945–11,948, 1985.

17

---

**Alfredo Lopez de Ar…, 5/31/2019 9:52 PM**
**Deleted:** This draft manuscript is distributed solely for purposes of scientific peer review. Its content is deliberative and pre-decisional, so it must not be disclosed or released by reviewers. Because the manuscript has not yet been approved for publication by the U.S. Geological Survey (USGS), it does not represent any official USGS finding or policy.

**Alfredo Lopez de Are…, 4/3/2019 3:32 PM**
**Deleted:** at http://geoport.whoi.edu/thredds/dodsC/sand/usgs/users/zdefne/run0x, where x stands for the run number

**Alfredo Lopez de Are…, 4/3/2019 3:32 PM**
**Deleted:** .

**Alfredo Lopez de Ar…, 3/21/2019 3:17 PM**
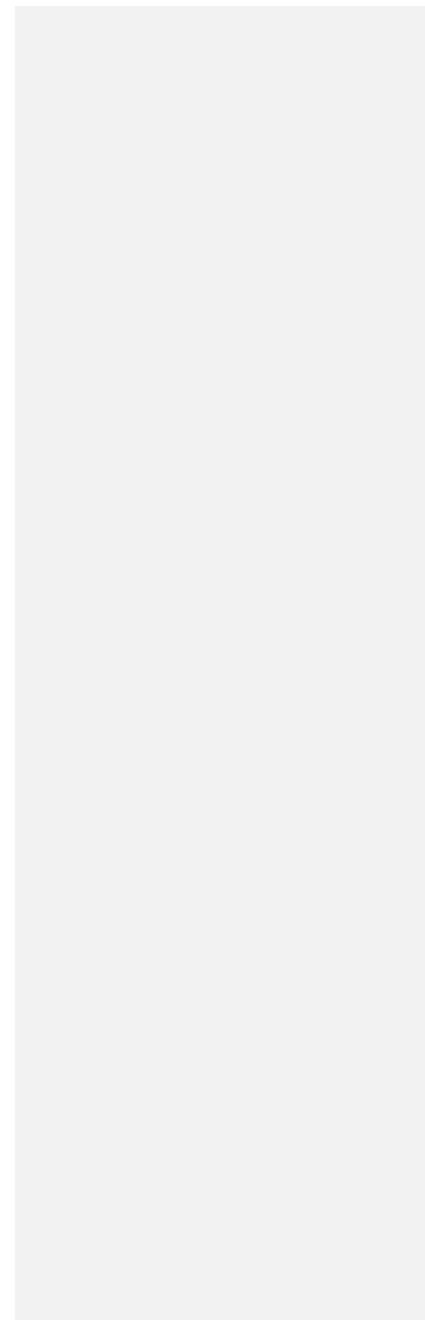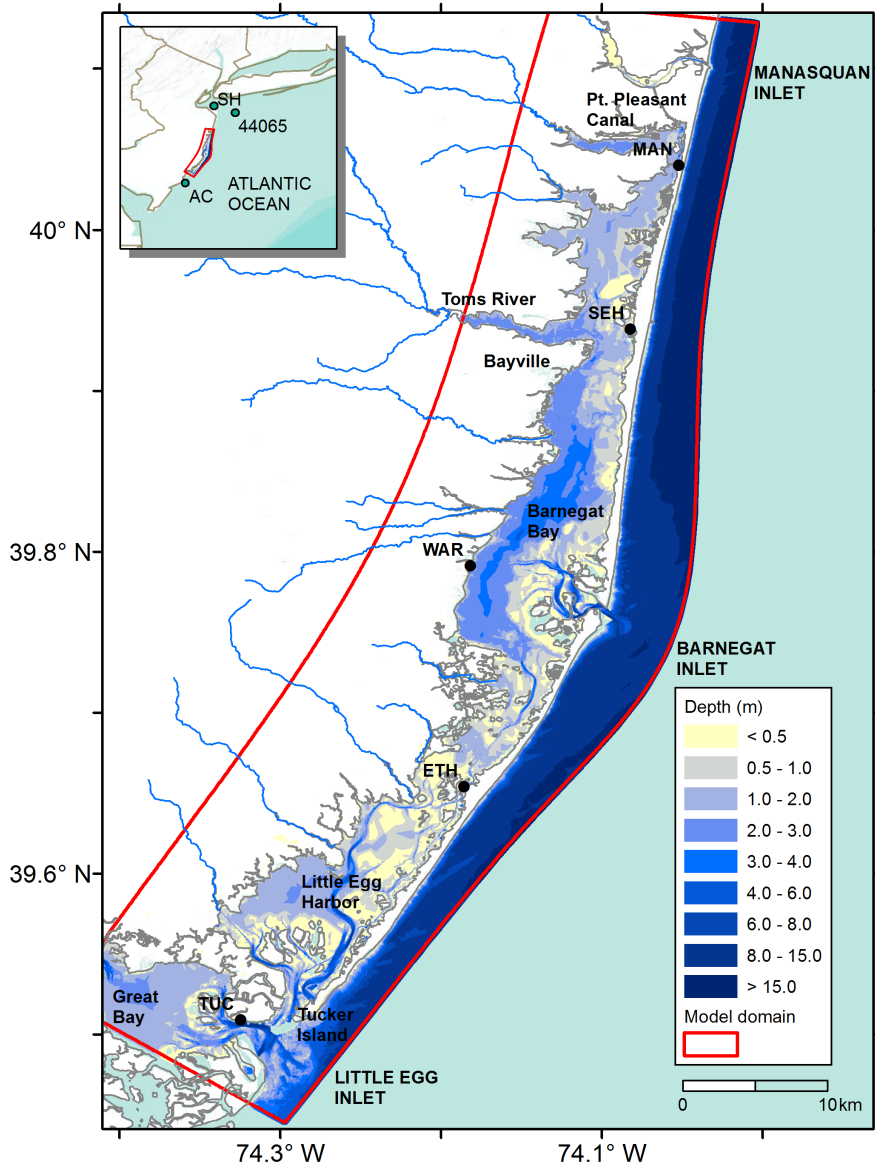**Deleted:** https://coawstmodel-trac.sourcerepo.com

**Alfredo Lopez de Ar…, 5/31/2019 9:52 PM**
**Formatted:** Hyperlink

525 Janzen, C. D., and Wong, K.-C.: Wind-forced dynamics at the estuary-shelf interface of a large coastal plain estuary, J. Geophys. Res., 107(C10), 3138, doi:10.1029/2001JC000959, 2002.

Keulegan, G. H.: Tidal flow in entrances: water-level fluctuations of basins in communication with seas, Committee on Tidal Hydraulics, Technical Bulletin No. 14, U.S. Army Corps of Engineers, Vicksburg, Miss., 89 pp., 1967.

Klein, R.J. and Nicholls, R. J.: Assessment of coastal vulnerability to climate change, Ambio, 182-187, 1999.

530 Kunreuther, H., Platt, R., Baruch, S., Bernknopf, R. L., Buckley, M., Burkett, V., Conrad, D., Davidson, T., Deutsch, K., Geis, D., and Jannereth, M.: The hidden costs of coastal hazards: Implications for risk assessment and mitigation, H. John Heinz III Center for Science, Economics, and the Environment. Panel on Risk, Vulnerability, and the True Costs of Coastal Hazards and H. John Heinz III Center for Science, Economics, and the Environment, 220 pp., Island Press, Washington, D. C., 2000.

535 Ludwig, K. A., Ramsey, D. W., Wood, N. J., Pennaz, A. B., Godt, J. W., Plant, N. G., Luco, N., Koenig, T. A., Hudnut, K. W., Davis, D. K., and Bright, P. R.: Science for a risky world—A U.S. Geological Survey plan for risk research and applications: U.S. Geological Survey Circular 1444, 57 pp., https://doi.org/10.3133/cir1444, 2018.

Mattingly, K. S., McLeod, J. T., Knox, J. A., Shepherd, J. M. and Mote, T. L.: A climatological assessment of Greenland blocking conditions associated with the track of Hurricane Sandy and historical North Atlantic hurricanes. International
540 Journal of Climatology, 35(5), 746-760, 2015.

McKenna, K. K., Farrell, S. C., and Gebert, J. A.: Hurricane Sandy: Beach-dune recovery at New Jersey Beach Profile Network (NJBPN) sites, Shore & Beach, 84(3), 5-17, 2016.

Neumann, B., Vafeidis, A.T., Zimmermann, J. and Nicholls, R.J.: Future coastal population growth and exposure to sea-level rise and coastal flooding-a global assessment. PloS one, 10(3), p.e0118571, 2015.

545 Nicholls, R.J., Wong, P. P., Burkett, V. R., Codignotto, J. O., Hay, J. E., McLean, R. F., Ragoonaden, S., and Woodroffe, C. D.: Coastal systems and low-lying areas. Climate Change 2007: Impacts, Adaptation and Vulnerability. Contribution of Working Group II to the Fourth Assessment Report of the Intergovernmental Panel on Climate Change, Parry, M. L., Canziani, O. F., Palutikof, J. P., van der Linden, P. J., and Hanson, C. E., Eds., Cambridge University Press, Cambridge, UK, 315-356, 2007.

550 Nicholls, R.J., Hanson, S.E., Lowe, J.A., Warrick, R.A., Lu, X. and Long, A.J.: Sea-level scenarios for evaluating coastal impacts. Wiley Interdisciplinary Reviews: Climate Change, 5(1), 129-150, doi:10.1002/wcc.253, 2014.

Pugh, D. T.: Tides, surges and mean sea-level. Wiley. ISBN 0 471 91505 X, 1987.

Rahmstorf, S.: Rising hazard of storm-surge flooding. Proceedings of the National Academy of Sciences, 114(45), 11806-11808, https://doi.org/10.1073/pnas.1715895114, 2017.

555 Reef, K. R., Lipari, G., Roos, P. C. and Hulscher, S. J.: Time-varying storm surges on Lorentz's Wadden Sea networks. Ocean dynamics, 68(8), 1051-1065, 2018

State Committee for the Zuiderzee: Verslag van de Staatscommissie Zuiderzee. Report. In Dutch, 1926.

18

Szpilka, C., Dresback, K., Kolar, R., Feyen, J., and Wang, J.: Improvements for the Western North Atlantic, Caribbean and Gulf of Mexico ADCIRC Tidal Database (EC2015), J. Mar. Sci. Eng, 4(4), p.72, doi:10.3390/jmse4040072, 2016.

560  Thieler, E. R., and Hammar-Klose, E. S.: National Assessment of Coastal Vulnerability to Sea-Level Rise: Preliminary Results for the US Atlantic Coast, Woods Hole, MA: United States Geological Survey (USGS), Open File Report 99-593, 1999.

U.S. Geological Survey, 2018, Coastal Change Hazards Portal web page, accessed October 30, 2018, at http://marine.usgs.gov/coastalchangehazardsportal/.

565  Vitousek, S., Barnard, P.L., Fletcher, C.H., Frazer, N., Erikson, L. and Storlazzi, C.D.: Doubling of coastal flooding frequency within decades due to sea-level rise. Scientific reports, 7(1), p.1399, 2017.

Wahl, T., Haigh, I.D., Nicholls, R.J., Arns, A., Dangendorf, S., Hinkel, J. and Slangen, A.B.: Understanding extreme sea levels for broad-scale coastal impact and adaptation analysis. Nature communications, 8, p.16075, 2017.

Warner J. C., Armstrong, B., He, R., and Zambon, J. B.: Development of a Coupled Ocean–Atmosphere–Wave–Sediment

570  Transport (COAWST) Modeling System, Ocean Modelling, 35, 230-244, doi: 10.1016/j.ocemod.2010.07.010, 2010.

Wilkin, J. L., and Hunter, E. J.: An assessment of the skill of real-time models of Mid-Atlantic Bight continental shelf circulation, J. Geophys. Res., 118 (6), 2919-2933, 2013.

Warner, J.C., Ganju, N., Sherwood, C.R., Kalra, T., Aretxabaleta, A, Olabarrieta, M., He, R., Zambon, J., and Kumar, N. (2019). A Coupled Ocean Atmosphere Wave Sediment Transport Numerical Modeling System (COAWST), USGS Github

575  Code Repository, https://code.usgs.gov/coawstmodel/COAWST.

Wong, K.-C., and DiLorenzo, J.: The response of Delaware's inland bays to ocean forcing, J. Geophys. Res., 93(C10), 12525–12535, 1988.

Wong, K.-C., and Moses-Hall, J. E.: On the relative importance of the remote and local wind effects to the subtidal variability in a coastal plain estuary, J. Geophys. Res., 103(C9), 18393–18404, 1998.

580  Wong, K.-C., and Wilson, R. E.: Observations of low-frequency variability in Great South Bay and relations to atmospheric forcing, J. Phys. Oceanogr., 14, 1893–1900, 1984.

19

Depth (m)

| | |
|---|---|
| | < 0.5 |
| | 0.5 - 1.0 |
| | 1.0 - 2.0 |
| | 2.0 - 3.0 |
| | 3.0 - 4.0 |
| | 4.0 - 6.0 |
| | 6.0 - 8.0 |
| | 8.0 - 15.0 |
| | > 15.0 |

Model domain

MANASQUAN INLET

Pt. Pleasant Canal

MAN

Toms River

SEH

Bayville

Barnegat Bay

WAR

BARNEGAT INLET

ETH

Little Egg Harbor

Great Bay

TUC

Tucker Island

LITTLE EGG INLET

SH

44065

ATLANTIC OCEAN

AC

40° N

39.8° N

39.6° N

74.3° W

74.1° W

0          10km

585 **Figure 1. Map of Barnegat Bay and Little Egg Harbor estuary showing the water level stations, bays, and inlets. The water level stations are: Tuckerton (TUC); East Thorofare (ETH); Waretown (WAR); Seaside Heights (SEH); and Mantoloking (MAN). Locations of offshore water level proxy stations and wind buoy are indicated in inset. COAWST model domain boundary is shown in red. Rte. 72 crosses the bay near ETH station and the breach that occurred during Hurricane Sandy was about a hundred meters away from MAN station, so they are not indicated in the map.**

Alfredo Lopez de Ar…, 5/31/2019 9:52 PM
**Deleted:** Tucketon

Alfredo Lopez de Ar…, 5/31/2019 9:52 PM
**Deleted:** Tucketon
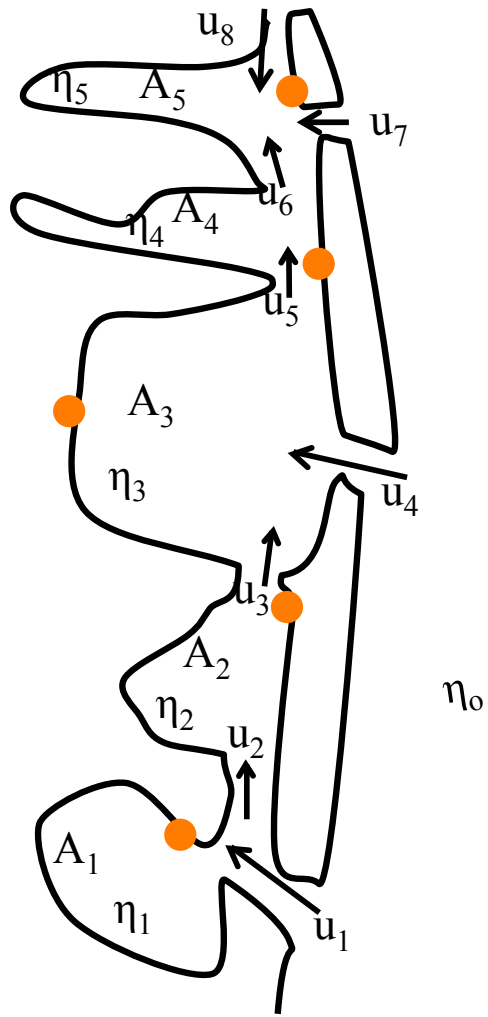
**Figure 2.** Schematic diagram of the ocean-inlet-bay system: $A_j$ is the surface area of the bays; $\eta_j$ the sea level in the bays; $\eta_o$ the sea level in the ocean; and $u_j$ is the velocity through channel j. The correspondence with the real bay system includes

595   areas from the bays (Great Bay, $A_1$; Little Egg Harbor, $A_2$; Barnegat Bay, $A_3$; Toms River sub-embayment, $A_4$; North of Mantoloking, $A_5$), flow through inlets (Little Egg Inlet, $u_1$; Barnegat Inlet, $u_4$; Point Pleasant Canal, $u_8$; and Mantoloking breach, $u_7$), and flow between bays (Tucker Island, $u_2$; Route 72, $u_3$; Bayville, $u_5$; Mantoloking, $u_6$). The location of the water level stations are indicated with dots and the names and specifications are in Figure 1 and Table 1.

23
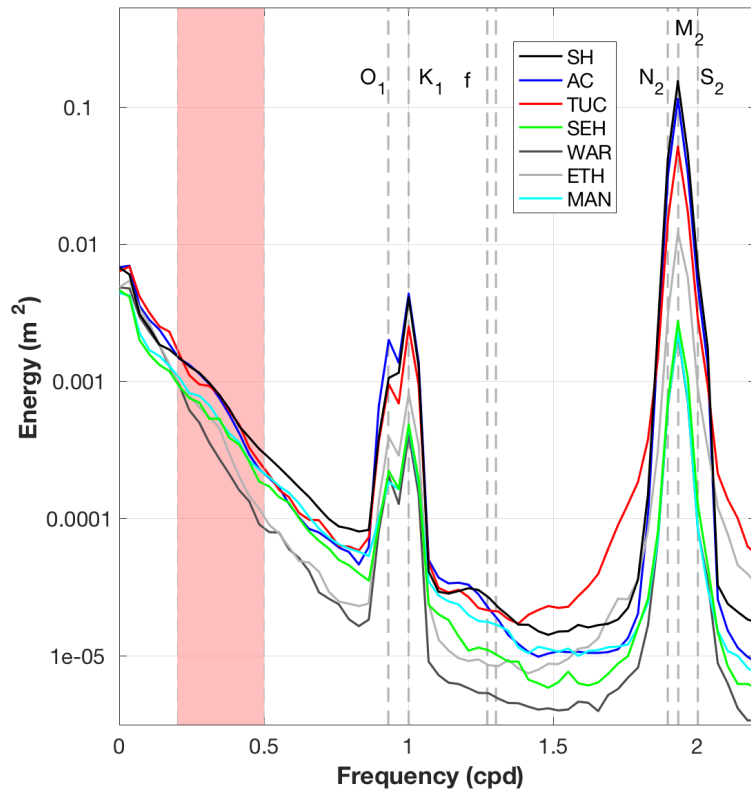
**Figure 3.** Energy spectra at all stations computed using a Hanning 29-day window with over-lapping (50%) data segments. $O_1$, $K_1$, $N_2$, $M_2$, and $S_2$ label the principal tidal frequencies and $f$ the inertial frequency. The vertical shaded area indicates the frequencies corresponding to the storm band (2-5 days). (cpd: cycles per day). See Table 1 for key to station abbreviations and Figure 1 for locations.

600

24
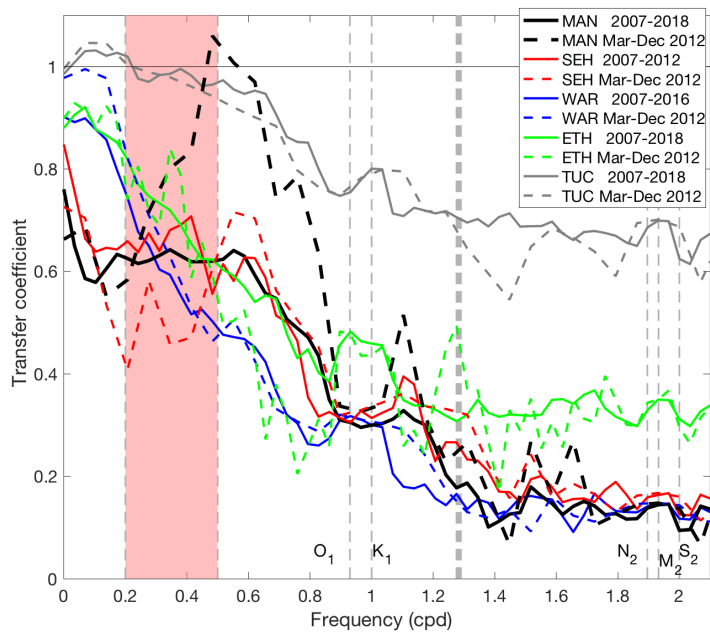
**Figure 4. Observed transfer from Atlantic City to 5 bay stations: Mantoloking (MAN), Seaside Heights (SEH), Waretown (WAR), East Thorofare (ETH), and Tuckerton (TUC). Solid lines indicate transfers for the entire available record at each station. Dashed lines represent observed transfers for the period March-December 2012, for which numerical model solutions were available. The vertical shaded area indicates the frequencies corresponding to the storm band (2-5 days).**

605
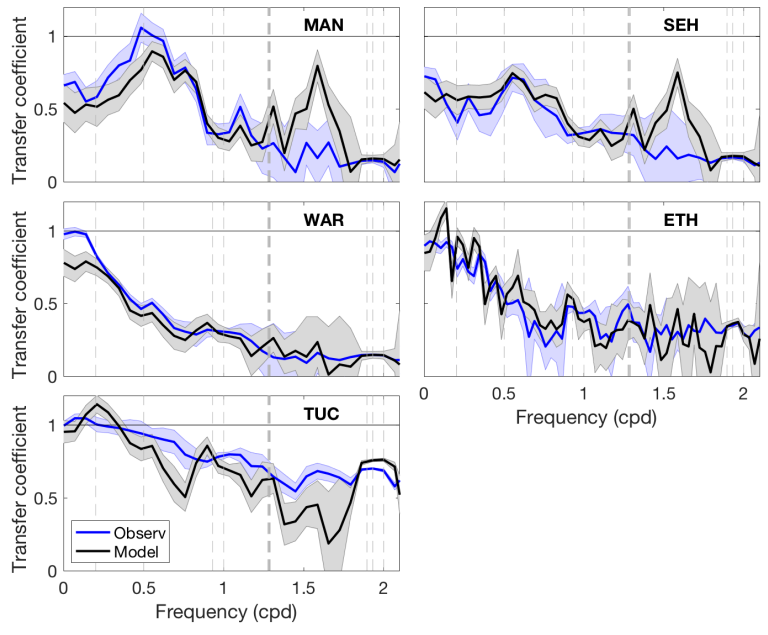
610

**Figure 5. Comparison between observed (blue) and numerical model (black) transfers for the period when both are available (March-December 2012) at five bay stations. Uncertainty envelopes for the transfer coefficient (Bendat and Piersol, 1986) are provided for observed (light blue) and model (gray) estimates.**
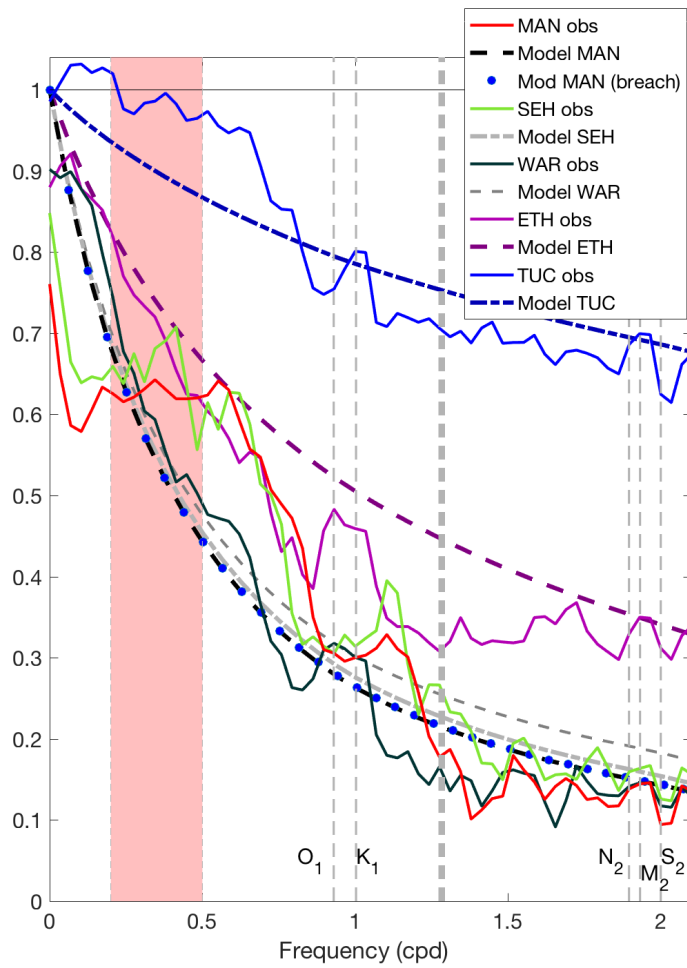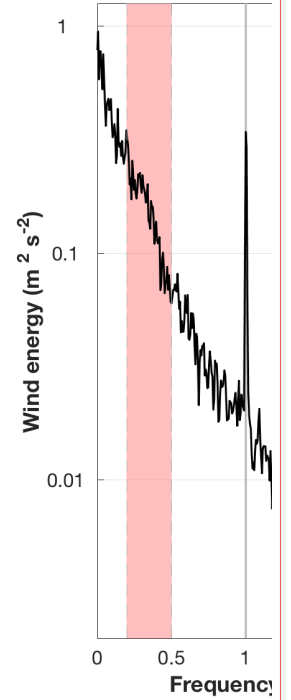
615

**Figure 6. Observed transfer for longest available record (solid lines) and best analytical model fit for each of the sub-embayments (dashed lines). The vertical shaded area indicates the frequencies corresponding to the storm band (2-5 days).**

27
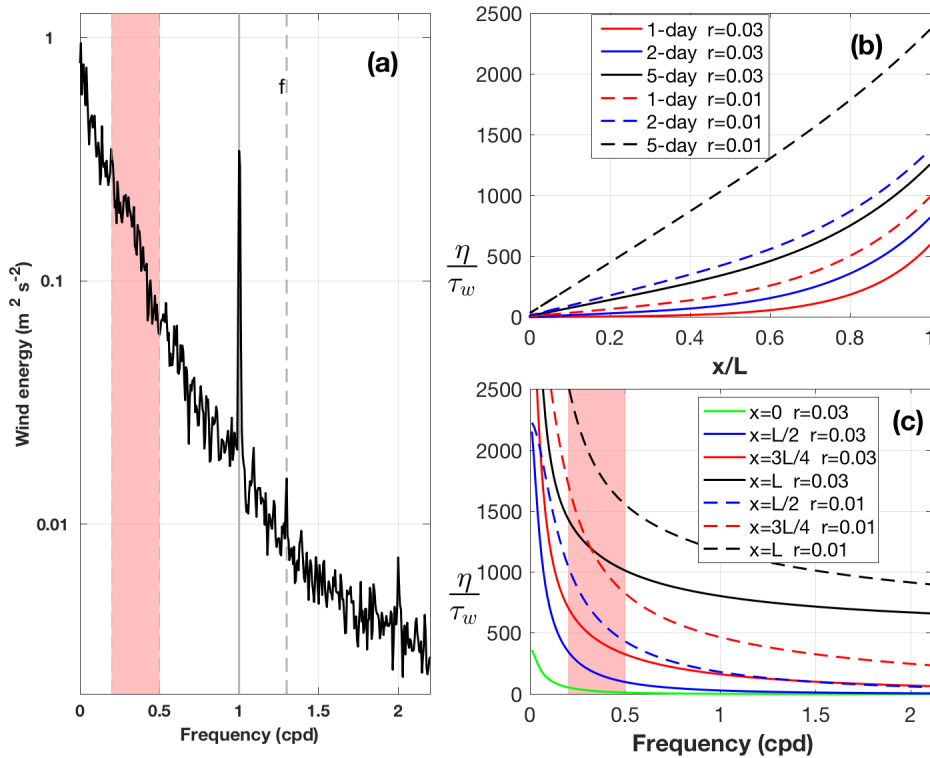
Figure 7: (a) Wind speed spectra for the along-bay wind component for NDBC 44065 buoy (2008-2018). (b) Kinematic wind stress contribution to local water level in the bay expressed as $\eta/\tau_w$ (m$^{-1}$s$^2$) following the Wong and Moses-Hall (1998) formulation as a function of distance from the southern edge of the bay. (c) Kinematic wind stress contribution to water level as a function of frequency. The vertical shaded area indicates the frequencies corresponding to the storm band (2-5 days).
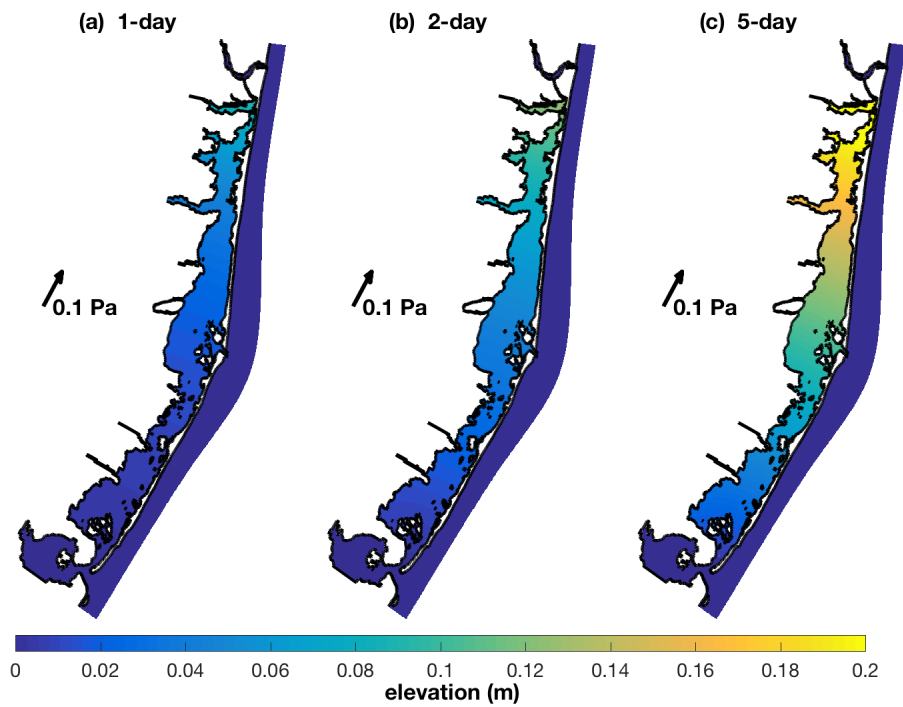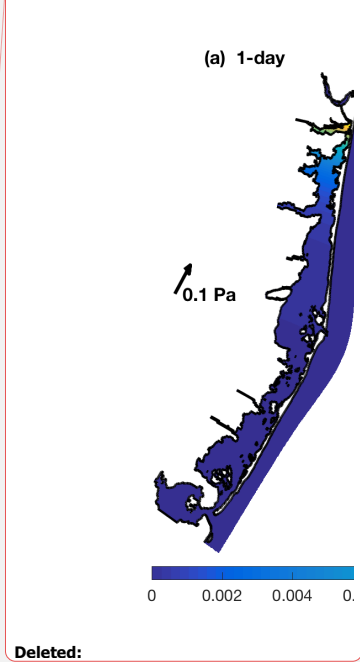
**Figure 8: Local wind setup inside the bay based on the Wong and Moses-Hall (1998) formulation for a wind stress of 0.1 Pa at specific periods: (a) wind with a 1-day period (e.g., sea breeze); (b) 2-day wind; and (c) 5-day wind.**

630
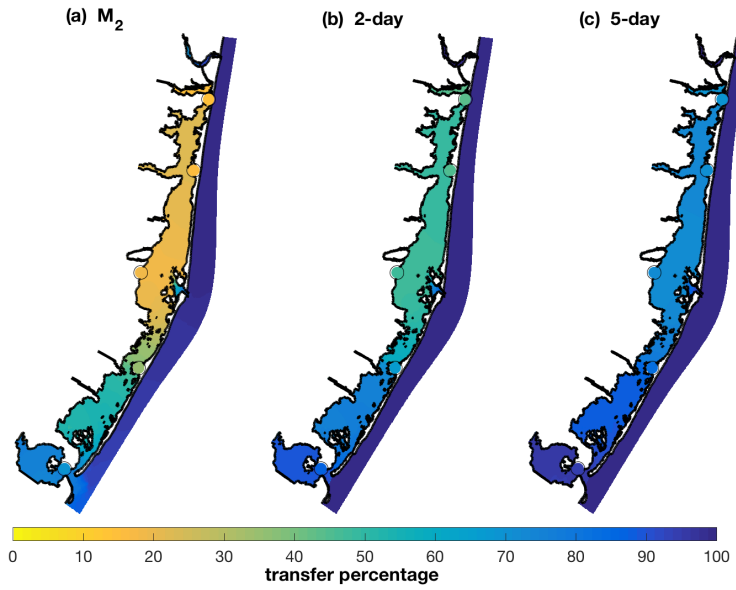
**Figure 9. Spatially variable transfer function (percentage) of offshore fluctuations transferred into the bays using Atlantic City as offshore proxy for three frequencies: (a) $M_2$ semidiurnal tide; (b) 2-day fluctuation in the storm band; and (c) 5-day fluctuation in the storm band. The filled circles represent the transfer estimate at each of the observed locations. Spatial pattern computed using the COAWST numerical solution.**

635
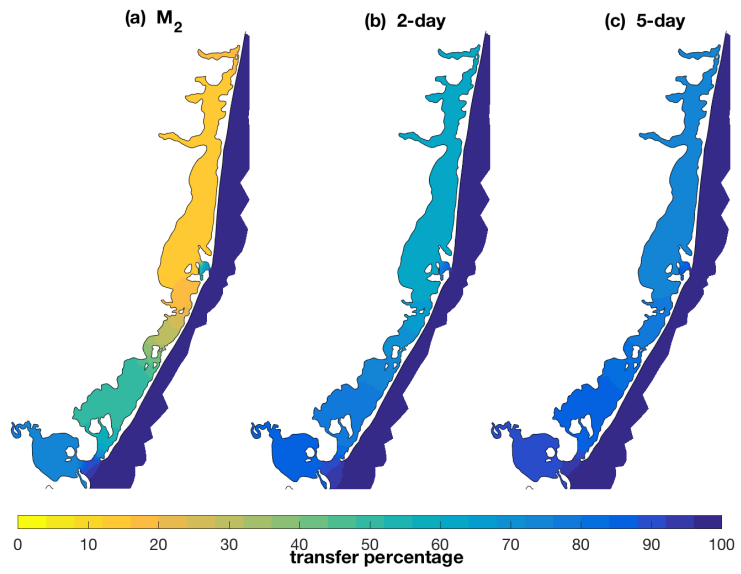
30

Figure 10: Transfer estimate based on ADCIRC tidal database for three frequencies: (a) M2 semidiurnal tide; (b) 2-day fluctuation in the storm band; and (c) 5-day fluctuation in the storm band.
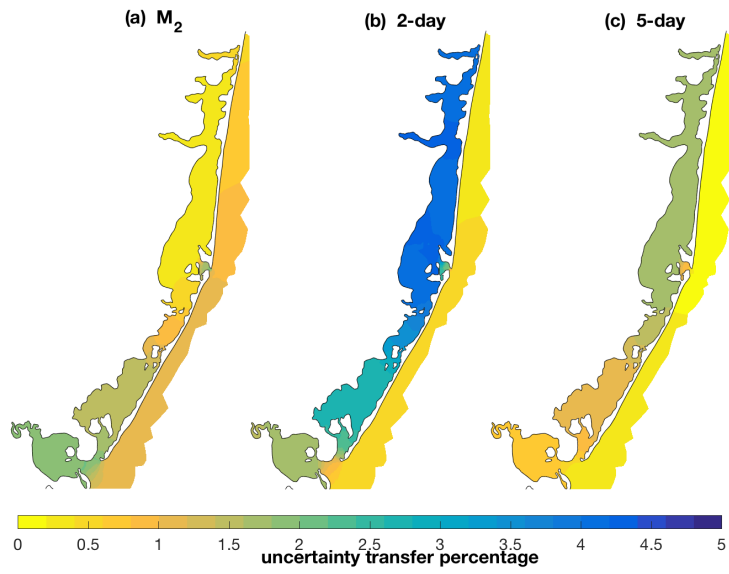
640

**Figure 11: Uncertainty in transfer estimate based on ADCIRC tidal database for three frequencies: (a) M2 semidiurnal tide; (b) 2-day fluctuation in the storm band; and (c) 5-day fluctuation in the storm band.**

32

645 **Table 1. Sites used in water level analysis. Check Figure 1 for locations. National Oceanic and Atmospheric Administration (NOAA); U.S. Geological Survey (USGS). Information on instrumentation type, sampling and quality control methodologies for the USGS stations is available starting at https://waterdata.usgs.gov/nwis/inventory.**

| Site name (Abbreviation) | Operator/ Site ID | Inlet/Bay | Available Period | Datum | Adjustment to NAVD88 |
|---|---|---|---|---|---|
| Sandy Hook, NJ (SH) | NOAA 8531680 | Offshore proxy | Jan 1910 – May 2018 | MSL | 0.15 m |
| Atlantic City, NJ (AC) | NOAA 8534720 | Offshore proxy | Aug 1911 – May 2018 | MSL | 0.12 m |
| Barnegat Bay at Mantoloking (MAN) | USGS 01408168 | Barnegat Bay | Oct 2007- May 2018 | NGVD29 | 0.34 m |
| Barnegat Bay at Seaside Heights (SEH) | USGS 01408750 | Barnegat Bay | Oct 2007- Oct 2012 | NGVD29 | 0.35 m |
| Barnegat Bay at Waretown (WAR) | USGS 01409110 | Barnegat Bay | Oct 2007- Dec 2016 | NGVD29 | 0.37 m |
| East Thorofare at Ship Bottom (ETH) | USGS 01409146 | Little Egg Harbor | Oct 2007- May 2018 | NGVD29 | 0.38 m |
| Little Egg Inlet near Tuckerton (TUC) | USGS 01409335 | Great Bay | Oct 2007- May 2018 | NGVD29 | 0.38 m |

**Table 2. Sum of energy ($m^2$) in the different bands of the spectra computed for the period 2007-2018 (or longest available record)**
650 **using a 29-day Hanning window with over-lapping (50%) data segments.**

| Site | Low frequency | 2-5 days | 1-2 days | Diurnal tide | 0.5-1 days | Semidiurnal tide | High frequency |
|---|---|---|---|---|---|---|---|
| **SH** | 0.023 | 0.007 | 0.002 | 0.008 | 0.001 | 0.251 | 0.002 |
| **AC** | 0.025 | 0.007 | 0.001 | 0.010 | 0.001 | 0.187 | 0.001 |
| **TUC** | 0.025 | 0.006 | 0.001 | 0.005 | 0.001 | 0.090 | 0.001 |

33

| | | | | | | | |
|---|---|---|---|---|---|---|---|
| **ETH** | 0.020 | 0.004 | 0.001 | 0.002 | <0.001 | 0.023 | 0.001 |
| **WAR** | 0.019 | 0.003 | 0.001 | 0.001 | <0.001 | 0.004 | <0.001 |
| **SEH** | 0.015 | 0.004 | 0.001 | 0.001 | <0.001 | 0.005 | <0.001 |
| **MAN** | 0.015 | 0.005 | 0.001 | 0.001 | <0.001 | 0.004 | <0.001 |